

SAFETY ANALYSIS REPORT

Chapter IX

For the

Penn State Breazeale Nuclear Reactor

By:

Daniel Hughes
Warren Witzig

Contributors:

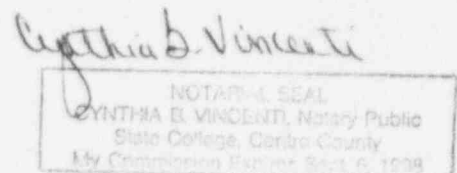
Patrick Boyle
Terry Flinchbaugh
Rodger Granlund
Samuel Levine
Pamela Stauffer
Marcus Voth

License Number R-2
Docket Number 50-05

The Pennsylvania State University
University Park, PA 16802

January 14, 1997 Rev. 1 (4/24/97)

9705020118 970428
PDR ADOCK 05000005
P PDR



SAFETY ANALYSIS REPORT

TABLE OF CONTENTS

Title Page	i
Table of Contents	ii
List of Figures	vii
List of Effective Pages	ix
I. INTRODUCTION	I-1
II. SITE CHARACTERISTICS	II-1
A. Geography and Demography II-1	II-1
1. Reactor Site Access Control	II-1
B. Nearby Industrial, Transportation, and Military Facilities	II-6
C. Meteorology	II-6
D. Geology and Hydrology	II-7
E. Seismology	II-10
F. References	II-10
III. REACTOR DESIGN	III-1
A. Introduction	III-1
B. Mechanical Design	III-1
1. Reactor Bridge	III-1
2. Reactor Suspension Tower	III-3
3. Reactor Grid Plates	III-3
4. Fuel-Moderator Elements	III-6
5. Control Rods	III-6
6. Control Rod Drives	III-9
7. Graphite Reflector Elements	III-16
C. Nuclear Design	III-16
1. Standard TRIGA Core	III-16
2. External Neutron Source	III-23
D. Thermal Design	III-23
IV. REACTOR POOL AND WATER SYSTEM	IV-1
A. Reactor Pool	IV-1
B. PSBR Water Handling System	IV-2
1. General	IV-2
2. Pool Recirculation Loop	IV-2
3. (DELETED)	IV-2

Cynthia B. Vincent
 NOTARIAL SEAL
 CYNTHIA B. VINCENT, Notary Public
 State College, Centre County
 My Commission Expires Sept. 9, 2001

TABLE OF CONTENTS

(Continued)

4. Transfer of Pool Water.....	IV-2
5. Heat Exchanger	IV-5
6. Liquid Waste Evaporator	IV-5
C. Water Quality Monitoring and Maintenance.....	IV-7
V. FACILITY CONSTRUCTION	V-1
A. Building	V-1
B. Heating and Ventilation.....	V-1
C. Utilities	V-6
D. Fire Protection	V-6
VI. FACILITIES AND EXPERIMENTERS	VI-1
A. Beam Ports.....	VI-1
B. D ₂ O Thermal Column	VI-4
C. Central Thimble	VI-4
1. Central Thimble Oscillator	VI-6
D. Verticle Tubes	VI-6
1. Jib Crane.....	VI-8
E. Pneumatic Transfer System	VI-8
1. Pneumatic Transfer System I.....	VI-8
2. Pneumatic Transfer System II.....	VI-12
F. Instrument Bridge	VI-14
G. Hot Cells	VI-14
H. Co-60 Irradiation Facility	VI-14
VII. REACTOR SAFETY, PROTECTION, CONTROL AND MONITORING SYSTEM	VII-1
A. System Summary	VII-1
B. System Design Philosophy	VII-6
C. Console Function Summary	VII-6
D. RSS Function Summary	VII-7
1. SCRAM Functions	VII-7
2. Interlock Functions	VII-7

TABLE OF CONTENTS (Continued)

E.	RSS Description.....	VII-8
1.	Wide Range Monitor Description	VII-10
2.	Power Range Monitor Description	VII-11
3.	Control and Alarm Subsystem Description	VII-12
a.	SCRAM and Control Logic Assembly Description	VII-12
b.	SCRAM and Rod Control Switch Assembly Description	VII-12
c.	SCRAM and Alarm Panel Assembly Description	VII-13
4.	The Power Distribution System.....	VII-13
F.	PCMS Function Summary	VII-13
1.	DCC-X Functions	VII-14
a.	Reactor Control and Regulation	VII-14
b.	Reactor Protection.....	VII-16
(a)	Reactor Stepback	VII-16
(b)	Reactor SCRAMs	VII-16
(c)	Reactor Interlocks	VII-17
(d)	Facilities Systems Support	VII-17
(i)	Emergency Evacuation	VII-17
(ii)	Reactor Operation Inhibit	VII-18
(iii)	Manual Controls	VII-18
(iv)	Operating History Records	VII-18
(v)	Police Services Notification	VII-18
(e)	Alarms	VII-19
(f)	Operator Interface	VII-19
(g)	Self Testing	VII-20
2.	DCC-Z Functions.....	VII-20
G.	Systems Operation Description	VII-20
1.	Reactor Safety System Description	VII-22
2.	RSS Relay Logic Design	VII-22
a.	SCRAM Logic.....	VII-24
b.	Transient Rod Air Interlock Logic	VII-25
c.	Rod Drive Interlocks.....	VII-26
H.	PCMS Hardware Description	VII-27
1.	Computers	VII-27
2.	Input/Output Hardware	VII-29
a.	Chassis Arrangement and Watchdog/Test Cards	VII-29
b.	Analog Signal I/O Cards	VII-30
c.	Digital Signal I/O Cards	VII-32
d.	Watchdog and I/O Self Test Circuits.....	VII-32

TABLE OF CONTENTS (Continued)

3. Motors and Associated Controllers	VII-33
a. Motor Control	VII-34
4. Power Supplies	VII-37
5. I/O Assignment	VII-37
I. PROTOL Generic Software Description	VII-39
1. Control Language	VII-39
2. The Operating System	VII-40
3. Generic Tasks Running in the PROTOL System	VII-41
4. System Self Checks and Defenses	VII-42
a. Defenses Against Loss of Field Sensor	VII-43
b. Defenses Against Loss of Power	VII-43
c. Defenses Against I/O Failure	VII-43
d. Defenses Against Computational Faults	VII-44
e. Defenses Against Program Corruption Faults	VII-44
5. DCC-X/DCC-Z Self Tests and Robustness Functions	VII-45
a. Self Tests on Start Up	VII-45
b. Self Tests While On Line	VII-46
J. Application Software	VII-48
1. Block Language Tasks	VII-48
2. Non-Block Language Tasks	VII-48
K. Control Room	VII-50
1. General Description	VII-50
2. Monitor Indications in the Control Room	VII-50
L. Minimum Safety SCRAMS and Interlocks	VII-53
M. References	VII-55
N. Glossary	VII-56
VIII. CONDUCT OF OPERATION	VIII-1
A. Organization and Responsibility	VIII-1
B. Reactor Operating Safety Philosophy	VIII-1
C. Training	VIII-3
D. Written Procedures	VIII-3
E. Records	VIII-4
F. Review and Audit of Records	VIII-4

TABLE OF CONTENTS

(Continued)

IX. SAFETY EVALUATION	IX-1
A. Introduction	IX-1
B. TRIGA Fuel Temperature Analysis of the Penn State Breazeale Reactor	IX-3
1. Steady State Analyses	IX-4
2. Pulsing Characteristics of the PSBR	IX-10
3. TRIGA Experiment to Measure Fuel Temperatures	IX-13
4. Evaluation of the Δt_g for Fuel Element I-14	IX-15
5. Evaluation of the Pulse Data for Fuel Element I-14.....	IX-19
6. Evaluation of the Fuel Element I-13 Temperature Data (Pulse and Steady State).....	IX-21
7. Conclusion (Temperature Analysis)	IX-23
C. Evaluation of the Limiting Safety System Setting (LSSS)	IX-25
D. Loss of Coolant Accident.....	IX-27
E. Maximum Hypothetical Accident (MHA)	IX-36
F. Reactivity Accident.....	IX-42
G. Conclusion	IX-43
H. References.....	IX-45

SAFETY ANALYSIS REPORT

LIST OF FIGURES

<u>Figure #</u>	<u>Title</u>
2-1	The Location of Centre County in Pennsylvania
2-2	Map of Centre County, Pennsylvania
2-3	The PSBR Site Boundary
2-4	Population Within a Five Mile Radius of the PSBR
2-5	The Physiography of Centre County
2-6	The Spring Creek Drainage Basin
3-1	The Location of the PSBR Core, Bridge, and Control Console
3-2	The Layout of the PSBR Grid Plates
3-3	The Arrangement of the PSBR Grid Plates and Safety Plate
3-4	A Standard TRIGA Fuel-Moderator Element
3-5	An Instrumented TRIGA Fuel Element
3-6	A Fueled Follower Control Rod with Respect to the PSBR Core
3-7	A Transient Control Rod
3-8	A Rack-and-Pinion Control Rod Drive
3-9	The Transient Rod Drive
3-10	Core Loading #1 Layout
3-11	Core Loading #4 Layout
3-12	A Graph of Peak Power Versus Prompt Reactivity for the First Nineteen Pulses with Core Loading #4
3-13	A Graph of Peak Fuel Temperature Versus Prompt Reactivity for the First Nineteen Pulses with Core Loading #4
3-14	A Layout of Core Loading #36
4-1	The PSBR Water Handling System
4-2	(DELETED)
4-3	The PSBR Heat Exchanger
4-4	The PSBR Liquid Waste Evaporating System
5-1	The Location of the PSBR on The Pennsylvania State University Campus
5-2a	The First Floor Plan of the Original Reactor Building
5-2b	The Ground Floor Plan of the Original Reactor Building
5-3	Location of the PSBR Electrical Supply Transformer
5-4a	The First Floor Location of Fire Extinguishers and Fire Alarm Boxes
5-4b	The Ground Floor Location of Fire Extinguishers and Fire Alarm Boxes
6-1	The Location of a Number of PSBR Facilities for Experimenters
6-2	The Location of the Beam Hole Laboratory, Hot Cells and Co-60 Irradiation Facility
6-3	The D ₂ O Thermal Column
6-4	The Central Thimble Oscillator
6-5	Pneumatic Transfer System I
6-6	Pneumatic Transfer System I Laboratory Terminus
6-7	Pneumatic Transfer System II
7-1	PSBR Console Layout
7-2	New PSBR Safety, Protection and Control System

LIST OF FIGURES (Continued)

<u>Figure #</u>	<u>Title</u>
7-3	Old PSBR Safety, Protection and Control System
7-4	Functional Block Diagram of RSS
7-5	PCMS and Interfaces to Other Systems
7-6	CMS Equipment Layout (Console Rear View)
7-7	Watchdog and I/O Self Test Circuits
7-8	Instrumentation Pedestal
7-9	Radiation Monitoring System
8-1	Organization Chart
9-1	PSBR Core Configuration Loading #36
9-2	Comparing Highest Measured Fuel Temperatures During a Pulse with EQ(34) for Fuel Element I-14
9-3	PSBR Core Configuration Loading #47
9-4	The Time Dependence of Air-Cooled Fuel Body for Center Element with 267 W Input
9-5	Summary of Equilibrium Data for LOCA Simulation Showing the Fuel-Element Cladding Temperature Versus Power Input to the Element for All Seven Dummy Elements Heated with the Same Power Input
9-6	Fuel/Cladding Temperature as a Function of Time After LOCA Initiation
9-7	Maximum Fuel Temperature Versus Power Density After LOCA for Various Cooling Times Between Reactor Shutdown and LOCA Initiation
9-8	Strength and Applied Stress as a Function of Temperature, U-ZrH _{1.65} Fuel with Fuel and Cladding the Same Temperature

SAFETY ANALYSIS REPORT

LIST OF EFFECTIVE PAGES

SAR - Title Page

Page i January 14, 1997

SAR - Table of Contents

Pages ii - vi January 14, 1997

SAR - List of Figures

Page vii-viii January 14, 1997

SAR - List of Effective Pages

Pages ix - x January 14, 1997 Rev. 1 (4/24/97)

SAR-I Introduction

Pages 1-2 March 1, 1985

SAR-II Site Characteristics

Pages 1-10 March 1, 1985

SAR-III Reactor Design

Pages 1-23 April 19, 1991

LIST OF EFFECTIVE PAGES (Continued)

SAR-IV Reactor Pool and Water System

Pages 1-2	April 19, 1991
Page 3	September 21, 1991
Pages 4-8	April 19, 1991
Page 9	March 1, 1985

SAR-V Facility Construction

Pages 1-4	March 1, 1985
Pages 5-6	April 19, 1991
Pages 7-10	March 1, 1985

SAR-VI Facilities and Experimenters

Pages 1-3	March 1, 1985
Page 4	September 21, 1992
Page 5-8	March 1, 1985
Pages 9-12	April 19, 1991
Pages 13-14	March 1, 1985

SAR-VII Reactor Safety, Protection, Control and Monitoring System

Pages 1-17	April 19, 1991
Page 18	September 21, 1992
Pages 19-49	April 19, 1991
Pages 50-54	February 28, 1992
Page 55	April 19, 1991
Page 56-57	August 23, 1991

SAR-VIII Conduct of Operation

Pages 1-2	April 19, 1991
Pages 3-4	June 7, 1993

SAR-IX Safety Evaluation

Pages 1-46	January 14, 1997 Rev. 1 (4/24/97)
------------	-----------------------------------

IX. SAFETY EVALUATION

A. Introduction

The Penn State Breazeale TRIGA Reactor (PSBR) was initially loaded with 8.5 wt% U-ZrH_{1.65} TRIGA fuel^(a) in December 1965.⁽²⁶⁾ The reactor core was operated with good performance with this fuel from 1965 through the early 1970's. It was then decided to strive to reduce fuel costs for the supplier, the Department of Energy (DOE), by achieving higher fuel burnup through an increased uranium concentration in the fuel. Fuel management studies at the PSBR performed in 1972^(1,2) showed, by analysis and experiment, that replacing some of the 8.5 wt% fuel with 12 wt% U-ZrH_{1.65} TRIGA fuel would achieve a better fuel utilization and a substantially lower fuel cost. The basic "in-out" fuel management method was selected as it would provide the necessary excess core reactivity to achieve a longer fuel burnup. This "in-out" method would start with 12 wt% U fuel being placed in some fuel locations in the center most ring, the B ring. The remainder of the core would be 8.5 wt% fuel. As the fuel was consumed, the partially burned 12 wt% fuel would be moved further out sequentially to the C and D rings while removing the 8.5 wt% fuel in those locations. New 12 wt% fuel would be fed into the B ring to replace fuel moved to outer fuel rings. In a given fuel location unburned 12 wt% fuel will produce a greater power density than the 8.5 wt% fuel by approximately 25 %. Thus, increased power density results in higher fuel temperatures which were studied⁽³⁻⁷⁾ analytically and experimentally to avoid exceeding safe operating conditions. The calculations agreed closely with the experimental data. Since 1972 the PSBR has been refueled with 12 wt% fuel.

On July 13, 1972 six 12 wt% fuel elements were placed in the B-ring replacing 8.5 wt% fuel which was moved to outer rings. This increased the core $k_{eff}^{(5)}$ to the level required for a larger fuel burnup and also increased the maximum measured fuel temperature to slightly over 400 °C, well below the safety limit of 1150 °C. The maximum radial power peaking factor was about 2.0 and the core reactivity increased by $1.624\% \frac{\Delta k}{k}$ (\$2.32). This reloading schedule of new fuel going into the B ring and after some fuel burnup being moved to the outer rings has been successful over the past 25 years requiring only 26 new 12 wt% fuel elements for the core.

In 1985 (Core Loading 38) a higher steady state maximum fuel temperature was observed (in an unburned instrumented fuel assembly of 12 wt%U, I-15) compared to previous similar instrumented (ie. I-13) fuel elements located in the same core position. The reason for this temperature increase is due to an increased fuel to fuel cladding gap. This was verified by comparing the peak fuel temperature of two similar instrumented fuel elements in the same core position subjected to the same sized pulse. The peak fuel temperature during a pulse of the two instrumented fuel elements were nearly the same whereas the steady state maximum fuel temperature was higher in the newer instrumented fuel element (I-15). Since the reactor pulse can be considered as an adiabatic process (the reactor pulse is << than the thermal time constant of the fuel), there is no instant heat transfer and the conductance of the gap between fuel and clad is immaterial. However under steady state conditions, the maximum fuel element temperature is a function of the gap conductance. Therefore with a larger gap, the fuel temperature will increase. In the case of I-15, there existed a larger fuel to fuel cladding gap prior to use than with I-13 after use.

^a From this point on in Chapter IX, fuel refers to U-ZrH_{1.65} TRIGA fuel with 20% nominal enrichment and zirconium to hydrogen atom ratio of 1 to 1.65 nominal.

It also has been found that the measured steady state maximum fuel temperature increases when the fuel element experiences increasing sizes of reactor pulses.^(25,26) Further use of the I-15 instrumented fuel element in larger pulses showed an increased steady state maximum fuel temperature. It is believed that the larger pulses produced a permanent strain in the fuel cladding due to the fuel thermal expansion. At the lower average steady state fuel temperature the fuel expansion is less than that occurring during the pulse, thus creating a fuel to fuel cladding gap. A new fuel management strategy has been developed to manage the sustained steady state fuel temperature.⁽²⁷⁾

The principal computer programs used to perform the calculations are PSU-LEOPARD⁽⁸⁾, EXTERMINATOR-2⁽⁹⁾, MCRAC⁽¹⁰⁾, and SCRAM⁽¹¹⁾. PSU-LEOPARD incorporates the standard LEOPARD⁽¹²⁾ computer program as originally received and adds additional subroutines. LEOPARD and PSU-LEOPARD calculate the group constants of the core as a function of burnup.

MCRAC is an automatic, multi-cycle, two-dimensional depletion code that gives the power distribution, k_{eff} , and isotopic inventory of the core at each burnup step. It is based on the flux and k_{eff} calculation performed by EXTERMINATOR-2, a multi-group two-dimensional diffusion theory code.

SCRAM is a multi-cycle depletion code created specifically for TRIGA reactors and adapted to the PSBR lattice design. It uses analytical equations to compute the power distribution, k_{eff} , and isotopic inventory for each cycle. The analytical equations are based on diffusion theory and the empirically fitted constants are derived using the PSU-LEOPARD, EXTERMINATOR-2, and MCRAC codes. In general, the calculations give good agreement with the measured power distributions and neutron fluxes.^(1,2,7) Any equivalent codes can be used as long as they are properly benchmarked.

The fact that one can calculate the power distribution with good accuracy is important to calculating the safety margin in PSBR operation. The calculations identify the fuel element having the maximum elemental power density, MEPD, in the core, and thus the one which will produce the highest fuel temperatures. This is true for both steady state and pulse operations.

The experimental and analytical studies which have been performed to show the safety margin in the operation of the PSBR are described in this section. In particular, the maximum measured fuel temperatures during steady state operation and pulse operation are mathematically related in a unique way to allow predictions of their values during the PSBR operation. All predictions indicate that the design and construction of the PSBR is such that the safety limit of the fuel will not be exceeded during steady state operation. Further, any pulse temperature of too large a magnitude can be prevented by reviewing the steady state temperature measurements prior to pulsing a large excess reactivity into the core as part of administrative control. This is also true for abnormal operating conditions. The following accidents are analyzed:

1. The loss of coolant accident.
2. The design basis accident which includes cladding rupture.
3. A reactivity accident.

The results of these analyses demonstrate that the reactor can continue to be operated safely within bounds of this safety analysis and the regulatory limits.

B. TRIGA Fuel Temperature Analysis of the Penn State Breazeale Reactor

There are two limiting conditions for establishing maximum allowed fuel temperatures. First, when the reactor is operating in the pool of water, the fuel temperature safety limit is 1150 °C. Under these conditions, the fuel cladding temperature is less than 500 °C and the cladding will not be ruptured by the internal hydrogen pressure.⁽¹³⁾ During a loss of coolant accident (LOCA), the fuel is not covered with water and must be air cooled. Secondly, when the fuel is air cooled, the cladding temperature will go above 500 °C, where the strength of the cladding decreases. Below a fuel temperature of 950 °C the hydrogen pressure will not rupture the cladding when the fuel and the cladding are the same temperature.⁽¹³⁾ Under these conditions, the fuel temperature safety limit is 950 °C.

Flux gradients across the fuel produce uneven temperature distributions. Pulsing a TRIGA fuel element to high power densities produces sudden expansion and contraction. During the rapid expansion phase, a large temperature gradient in the radial direction can cause uneven axial expansion producing a transverse bend. Experience with the TRIGA fuel elements has shown that they can receive thousands of pulses without being damaged provided their temperature limits are not exceeded. TRIGA fuel elements are considered damaged and no longer useable if their cladding has been ruptured or their dimensions change to where the transverse bend exceeds 0.125 inches over the length of the cladding or the length increases 0.125 inches.

The temperature profile in a single TRIGA fuel element is a function of its fuel and fission product distribution and is different for pulse operation compared to steady state operation. During steady state operation, the maximum fuel temperature is at the central fuel-zirconium rod interface. Since the thermocouple is placed near this interface, the measured fuel temperature is close to the maximum fuel temperature⁽⁴⁾ (the maximum fuel temperature has been analytically determined to be no more than 5% more than the measured fuel temperature). During a pulse, the maximum fuel temperature is near the fuel-cladding interface and the measured fuel temperature is no less than 60-65% of the maximum fuel temperature.⁽⁴⁾ To know what limits to place on operation, it is important to understand the TRIGA fuel temperature distribution in a fuel element during steady state and pulse operation and to relate the measured fuel temperature to the maximum fuel temperature.

An instrumented TRIGA fuel element is built with three thermocouples placed 0.0226 ft radially from the center, but spaced vertically 1 inch apart. The middle thermocouple is in the midplane of the fuel region of the TRIGA fuel element. The thermocouple measures the fuel temperature at a specific point within the fuel element which is not the maximum fuel temperature for pulse operation. During a pulse, the temperature distribution is the same as that of the volumetric thermal source strength, $q'''(\mathbf{r})$, so that the peak fuel temperature is near the fuel cladding interface. This is due to self-shielding within the fuel. As a result, the measured fuel temperature can be significantly lower than the maximum fuel temperature. On the other hand, the peak fuel temperature during steady state operation is at the inner boundary of the fuel; thus, the measured fuel temperature is slightly less than the maximum fuel temperature. The measured fuel temperature in an 8.5 wt% U fuel element is closer to the maximum temperature than it is in a 12 wt% U fuel element because the self-shielding of the 12 wt% U fuel U is greater than the 8.5 wt% U fuel thereby producing a $q'''(\mathbf{r})$ with a steeper gradient.

The temperature distribution within the fuel can be calculated from a knowledge of fuel geometry, heat transport parameters, and $q'''(\underline{r})$ as shown by Haag and Levine.⁽³⁾ The volumetric thermal source strength in a fuel element is a function of the core power, the core configuration, and the element's position within the core. For any core configuration, $q'''(\underline{r})$ can be determined by neutronic analysis and then used to determine the peak temperature during a pulse or during steady state operation. The steady state fuel temperature is determined by the boundary conditions at the cladding water interface and the value of $q'''(\underline{r})$. Studies performed by Haag and Levine have shown that subcooled boiling takes place in the PSBR when the TRIGA core exceeds 200 kW. This helps limit the temperature rise of the cladding surface temperature, t_c , because when boiling occurs t_c increases proportional to approximately $(q'')^{0.33}$.⁽¹⁴⁾ Hence, the heat flux, q'' , must increase by a factor of 8 to increase the difference between t_c and the water saturation temperature by a factor of 2.

It is important to recognize that the $q'''(\underline{r})$ produced in a fuel element for a particular core configuration is the heat source that establishes the fuel temperature for both steady state operation and pulse operation. Hence, there is a direct relation between the measured fuel temperature at steady state and during pulse operation for the same core configuration and fuel element. The fuel temperature measured in the fuel element having the highest power density in the core during steady state operation can be used to determine the maximum fuel temperature in the core during a pulse. This relationship is described in this section.

1. Steady State Analyses

Standard heat transport calculations are used to analyze the steady state fuel temperatures for the PSBR.

Let

$$\begin{aligned} q'''_j(\underline{r}) &= \text{volumetric thermal source strength at position } \underline{r} \text{ within the } j^{\text{th}} \text{ region.} \\ P_j &= \text{power generated by the } j^{\text{th}} \text{ fuel element.} \end{aligned}$$

Then

$$P_j = \int_V q'''_j(\underline{r}) dV, \quad (1)$$

where the integral is over the fuel volume, V , of the j^{th} fuel element. The average power, \bar{P} , produced by a fuel element in the core, and the normalized power for the j^{th} fuel element, NP_j , are related to P_j by the expression

$$P_j = \bar{P} NP_j, \quad (2)$$

A core of N_c fuel elements producing a total power of Q can be expressed as

$$Q = N_c \bar{P} = N_c \bar{q}''' V, \quad (3a)$$

and

$$\bar{P} = \frac{Q}{N_c} = \bar{q}''' V, \quad (3b)$$

where \bar{q}''' is the volumetric thermal source strength averaged over all fuel in the core, and N_c is the number of fuel elements in the core.

It can be immediately observed that operating at 1 MW, implies that for a core with $N_c = 90$, then $\bar{P} = 0.0111$ MW, and for a core with $N_c = 100$, then $\bar{P} = 0.010$ MW.

Using Goodwin's⁽¹⁵⁾ measured $q_j'''(r, z)$ as

$$q_j'''(r, z) = (A_o + B_o r^2) \bar{q}_j'''(z), \quad (4)$$

where for the j^{th} fuel element

$$\int_V q_j'''(r, z) dV = \bar{q}_j''' V, \quad (5)$$

z is the axial position along the j^{th} fuel element, and A_o and B_o are constants. A thermocouple is located at the fuel midplane where $z = 7.5$ ". The length of the fuel is 15". Thus, at the fuel midplane,

$$q_j'''(r, 7.5) = q_{oj}'''(r) = \bar{q}_{oj}'''(A_o + B_o r^2), \quad (6)$$

and

$$\bar{q}_{oj}''' = f_a \bar{q}_j''' = f_a N P_j \bar{q}''' = f_a N P_j \frac{\bar{P}}{V}, \quad (7)$$

where f_a is the axial peaking factor. The following definitions are used for the j^{th} fuel element in these equations:

$$\begin{aligned} q_j'''(r, z) &= \text{point volumetric thermal source strength,} \\ \bar{q}_j''' &= \text{volumetric thermal source strength averaged} \\ &\quad \text{over the radial direction,} \\ \bar{q}_j''' &= \text{volumetric thermal source strength averaged} \\ &\quad \text{over the fuel volume.} \end{aligned}$$

When the j^{th} subscript is missing, \bar{q}''' and \bar{q}''' refer to the fuel element producing an average power in the core.

For the j^{th} fuel element

$$P_j = \bar{q}_j''' V, \quad (8a)$$

and

$$\bar{q}_j''' = \frac{\bar{P}}{V}. \quad (8b)$$

Equation (8a) can be written, using Equation (2), in the following form:

$$P_j = NP_j \bar{q}_j''' V. \quad (9)$$

The temperature rise between the fuel and the cladding at the fuel element midplane during steady state operation is directly dependent on $\bar{q}_j'''(r)$. Dropping the j subscript for convenience but remaining in the fuel midplane

$$\frac{1}{r} \frac{1}{dr} \left[k_r r \frac{dt}{dr} \right] = -\bar{q}_o''' (A_o + B_o r^2), \quad r_z \leq r \leq R, \quad (10)$$

where

$$\begin{aligned} r_z &= \text{radius of Zr rod in the center of the fuel rod,} \\ R &= \text{radius of the fuel rod.} \end{aligned}$$

Integrating Equation (10) gives

$$t(r) - t_s = \frac{\bar{q}_o'''}{2k_f} \left[\frac{A_o}{2} (R^2 - r^2) - A_o r_z^2 \ln \frac{R}{r} + \frac{B_o}{8} (R^4 - r^4) - \frac{B_o r_z^4}{2} \ln \frac{R}{r} \right], \quad (11)$$

All parameters in Equation (11) are described and given in Table 9-1. Substituting the values for the parameters into Equation (11) gives, for the thermocouple temperature, t_{tc} ,

$$t_{tc} - t_s = 6.039 \times 10^{-5} \bar{q}_o''', \quad (12a)$$

Substituting Equation (7) into Equation (12a) and returning to the j^{th} fuel element gives

$$(t_{tc} - t_s)_j = 6.039 \times 10^{-5} \frac{t_a \bar{P}}{V} NP_j, \quad (12b)$$

Using $Q = 1 \text{ MW}$ in Equation (3b),

$$\bar{P} = \frac{1}{N_c} 3.412 \times 10^6 \frac{\text{BTU}}{\text{hr}}, \quad (13)$$

Table 9-1

Parameters for the 12 wt% U-ZrH TRIGA Fuel Elements
(Enriched to less than 20% ^{235}U)

Thermocouple radius, R_{tc}	0.0226 ft [†]
Fuel mean radius, R	0.0596 ft [†]
Zr rod radius, r_z	0.0079 ft [†]
Cladding thickness, C	0.00165 ft
Fuel element radius, $R + C$	0.06125 ft [†]
Conductivity cladding, k_c	9.5 Btu/hr ft ² °F
Conductivity fuel, k_f	10.5 Btu/hr ft ² °F
Core average volumetric thermal source strength, \bar{q}'''	2.49×10^8 $\frac{\text{Btu}}{\text{hr ft}^3}$
A_0 (12 wt% U fuel new) (Reference 4)	0.6534
B_0 (12 wt% U fuel new) (Reference 4)	202 ft ⁻²
Number of elements, N_c (Loading 36)	94.6
Number of elements, N_c (Loading 45T)	88
Axial peaking factor, f_a	1.25*
Prompt temperature coefficient, α (Ref. 19)	-1.4×10^{-4} $\delta k/k/^\circ\text{C}$
C_f (Loading 36) Correction Factor	0.98**

* This value is used for analyses subsequent to the original SAR since it is a more typical value used for TRIGA reactors.

** See the description of this factor in the text immediately after Equation (15).

[†] These are nominal values and may vary with the manufacturers specification. It is also assumed that the fuel - cladding gap is zero (0) which in general is not true.

The volume of fuel in a TRIGA fuel element is

$$V = \pi(R^2 - r_z^2)H,$$

where H is the fuel height. Using $H = 1.25$ ft and the value from Table 9-1 for the other parameters

$$V = 1.37 \times 10^{-2} \text{ ft}^3, \quad (14)$$

Substituting Equations (13) and (14) into Equation (8b) gives

$$\bar{q}''' = C_f \frac{2.49 \times 10^8 \text{ BTU}}{N_c \text{ hr ft}^3}, \quad (15)$$

where C_f is a correction factor for setting the power instrument to read 1 MW when the actual power is reduced by the factor $(1 - C_f)$. This reduction is to provide an extra margin of safety to compensate for an uncertainty in calibration. What value is used for C_f depends on how the equations are being used. If they are being used to predict fuel temperature from a given NP, a more conservative $C_f = 1$ should be used. If the equations are being used to determine NP from measured fuel temperature, a $C_f \leq 1$ may be used depending on the confidence the experimenter has in the accuracy of the power calibration.

Equation (12b) can now be written as:

$$(t_{fc} - t_s)_f = 1.5 \times 10^4 C_f \frac{f_a NP_f}{N_c} \text{ } ^\circ\text{F}, \quad (16)$$

$$(t_{fc} - t_s)_f = 8.33 \times 10^3 C_f \frac{f_a NP_f}{N_c} \text{ } ^\circ\text{C},$$

The measured fuel temperature, t_{fc} , depends on the temperature at the cladding surface in the fuel midplane, t_c . Because of subcooled boiling above 200 kW, this temperature rises very slowly. The Δt is proportional to $(q''')^{0.33}$, where Δt is the difference between t_c and the coolant saturation temperature.⁽¹⁴⁾ As a result, it is assumed that the surface cladding is superheated by a fixed Δt degrees and thus at 1 MW, $t_c = 140$ °C. This should be correct within ± 10 °C at 1 MW for all NP_f's greater than 1 and less than 3. We may write

$$t_{fcf} = (t_{fc} - t_s)_f + (t_s - t_c)_f + t_c, \quad (17)$$

where the first term on the right hand side of Equation (17) is evaluated using Equation (16). The second term, the temperature change between the fuel cladding and the surface of the fuel rod, is derived assuming a gap, g , between the cladding and the fuel. Solution of the standard heat equation gives for

$$(t_s - t_c)_f = (t_s - t_g)_f + (t_g - t_c)_f, \quad (18a)$$

the following equation:

$$(t_s - t_c)_l = \frac{q_{oj}'}{2\pi k_g} \ln \frac{R+g}{R} + \frac{q_{oj}'}{2\pi k_c} \ln \frac{R+g+C}{R+g}, \quad (18b)$$

where

- t_s = temperature of the fuel at the fuel cladding interface
- t_g = temperature of the cladding facing the gap
- k_g = conductivity of the gap
- k_c = conductivity of the cladding
- C = thickness of the cladding
- g = thickness of the gap
- q_{oj}' = linear heat generation rate

and the other parameters are as previously defined.

Thus

$$(t_s - t_g)_l = \frac{q_{oj}'}{2\pi k_g} \ln \frac{R+g}{R}, \quad (19a)$$

and

$$(t_g - t_c)_l = \frac{q_{oj}'}{2\pi k_c} \ln \frac{R+g+C}{R+g} \equiv \frac{q_{oj}'}{2\pi k_c} \ln \frac{R+C}{R}, \quad (19b)$$

Equation (19a) will be evaluated experimentally as described later, whereas Equation (19b), the temperature drop across the cladding, can be evaluated from the physical values of the parameters.

By definition

$$q_{oj}' = \pi(R^2 - r_z^2) \bar{q}_{oj}''' = \pi(R^2 - r_z^2) f_a NP_l \bar{q}''', \quad (20)$$

Assuming an average core temperature drop across the gap, $\bar{\Delta t}_g$, Equation (19a) becomes

$$(t_s - t_g)_l = C_l f_a NP_l \bar{\Delta t}_g, \quad (21a)$$

where

$$\bar{\Delta t}_g = \frac{R^2 - r_z^2}{2k_g} \bar{q}''' \ln \frac{R+g}{R}. \quad (21b)$$

Also, Equation (19b) becomes, using Equation (20)

$$(t_g - t_c)_l = \frac{R^2 - r_z^2}{2k_c} f_a NP_l \bar{q}''' \ln \frac{R+C}{R}. \quad (21c)$$

Using the values of Table 9-1, Equation (21c) reduces to

$$(t_g - t_c)_I = 1.248 \times 10^3 C_f \frac{f_a NP_I}{N_c} \text{ } ^\circ\text{F}, \quad (21d)$$

$$(t_g - t_c)_I = 6.936 \times 10^2 C_f \frac{f_a NP_I}{N_c} \text{ } ^\circ\text{C}.$$

Substituting Equations (21a) and (21d) into Equation (18a), and using the result in Equation (17), it follows that

$$t_{icj} = \left(\frac{9.024 \times 10^3}{N_c} + \overline{\Delta t_g} \right) C_f f_a NP_I + 140 \text{ } ^\circ\text{C}. \quad (22)$$

Equation (22) is used to calibrate an instrumented 12 wt% U fuel element to provide a measured fuel temperature, t_{ic} , during steady state operation.

2. Pulsing Characteristics of the PSBR

The temperature distribution in a TRIGA fuel element during a pulse has the same distribution as expressed in Equation (4) up to 89% of the fuel radius.⁽¹⁵⁾ It has been found that adiabatic conditions hold up to 0.07 sec. during which time the maximum fuel temperature is reached.⁽¹⁵⁾ Using the values of Table 9-1, it is found⁽⁴⁾ that the maximum fuel temperature during a pulse is 1.6 times that measured by the thermocouple. Thus, during the pulse, the shape of the temperature distribution in a fuel element remains constant, but the magnitude quickly rises. What we are concerned with here is the maximum fuel temperatures reached during the pulse. To prevent confusion, we use the term highest maximum fuel temperature to refer to the highest temperatures reached at any point within the fuel element during the pulse. The highest maximum fuel temperature is thus the maximum fuel temperature reached during a pulse and must remain below 1150 °C. However, the highest measured fuel temperature is 1/1.6 or 0.625 times the highest maximum fuel temperature which corresponds to a measured fuel temperature of 720 °C. Thus, setting the Limiting Safety System Setting (LSSS) at 650 °C, corresponds to a maximum fuel temperature of 1040 °C. The LSS scram will have no effect on the maximum fuel temperature reached during a pulse because the instrumentation time lag allows the peak to be reached before a scram can occur. The maximum fuel temperature reached during a pulse must be limited by the magnitude of the prompt excess reactivity insertion (δk_p) and/or the $q'''(r)$ produced in a fuel element for a particular core configuration.

A semi-empirical equation, Equation (29), is developed using the definition of the prompt temperature coefficient. The large negative prompt temperature coefficient, α , provides the TRIGA core with its pulsing capability. When excess k_{eff} , $\delta k_{ex} = k_{eff} - 1$, is inserted into the reactor, the reactor will go on a prompt period, provided

$$\delta k_p = \delta k_{ex} - \beta, \quad (23)$$

is positive, i.e., $\delta k_p > 0$. β is the effective delayed neutron fraction (0.007).

Let:

- $\bar{\delta t}_p =$ maximum fuel temperature rise averaged over the total core fuel volume for a pulse.
 $\bar{\delta t}_{poj} =$ maximum fuel temperature rise averaged over the radius of the j^{th} fuel element at its midplane.
 $\alpha =$ prompt temperature coefficient of reactivity of the TRIGA core.

The prompt temperature coefficient is defined as:

$$\alpha = -\frac{\delta k_p}{\bar{\delta t}_{pp}}, \quad (24a)$$

or

$$\bar{\delta t}_{pp} = -\frac{\delta k_p}{\alpha}, \quad (24b)$$

where

- $\delta k_p =$ prompt excess reactivity insertion.
 $\bar{\delta t}_{pp} =$ average maximum rise in core fuel temperature due to the prompt excess reactivity insertion.

Equation (24b) does not include the average core temperature rise due to a pulse insertion of \$1 excess reactivity, δt_{p1} . Thus, the total average fuel temperature rise during a pulse, $\bar{\delta t}_p$, is:

$$\bar{\delta t}_p = \bar{\delta t}_{pp} + \bar{\delta t}_{p1}. \quad (25a)$$

For the j^{th} fuel element, its corresponding temperature increase in the midplane is

$$\bar{\delta t}_{poj} = f_a NP_j \bar{\delta t}_p, \quad (25b)$$

or

$$\bar{\delta t}_{poj} = f_a NP_j \left(-\frac{\delta k_p}{\alpha} \right) + f_a NP_j \bar{\delta t}_{p1}. \quad (25c)$$

Initially the core fuel temperature is that of the pool water, T_o , and during the pulse an adiabatic increase in temperature, $\delta t_{poj}(r)$, is assumed. Hence,

$$\delta t_{poj}(r) = \bar{\delta t}_{poj} (A_o + B_o r^2). \quad (26a)$$

Equation (26a) expresses the maximum temperature rise above room temperature for the j^{th} fuel element as a function of fuel radius. For convenience

$$\delta t_{poj}(r) = \bar{\delta t}_{poj} f(r), \quad (26b)$$

where

$$f(r) = A_o + B_o r^2. \quad (26c)$$

The temperature in the midplane of the fuel element at any r position, $t_{poj}(r)$ can be expressed as:

$$t_{poj}(r) = \bar{\delta t}_{poj} f(r) + T_o. \quad (27a)$$

Let

$$t_{poj} = \text{maximum pulse temperature measured by the thermocouple in the } j^{\text{th}} \text{ fuel element.}$$

Then

$$t_{poj} = \bar{\delta t}_{poj} f(r_{ic}) + T_o. \quad (27b)$$

Using the values of Table 9-1

$$t_{poj} = 0.7566 \bar{\delta t}_{poj} + T_o. \quad (27c)$$

Substituting Equation (25c) into Equation (27c)

$$t_{poj} = 0.7566 \left[f_a NP_j \left(-\frac{\delta k_p}{\alpha} \right) + f_a NP_j \bar{\delta t}_{p1} \right] + T_o \quad (28)$$

Equation (28) is used as the basis for developing the semi-empirical equation, Equation (29), to fit the actual pulse data as a function of NP_j , i.e.,

$$t_{poj} = K_{14} f_a NP_j \left(-\frac{\delta k_p}{\alpha} \right) + f_a NP_j \bar{\delta t}_{p0} + T_o, \quad (29)$$

where K_{14} and $\bar{\delta t}_{p0}$ are empirical constants to be determined experimentally. The experimental data may also be represented by:

$$t_{poj} - T_o = M_j \delta k_p + b_j, \quad (30)$$

where

$$M_j = \frac{K_{14} f_a NP_j}{-\alpha}, \quad (31a)$$

and

$$b_j = f_a NP_j \overline{\delta t_{po}}. \quad (31b)$$

NP_j and $\overline{\delta t_{po}}$ are determined by fitting the experimental data to Equation (30) where NP_j , f_a , and α are known. In Equation (30), $M_j \delta k_p$ represents the temperature rise during a pulse due to the prompt excess reactivity (δk_p) insertion and b_j represents the corresponding temperature rise due to the $\$1$ excess reactivity insertion.

3. TRIGA Experiment to Measure Fuel Temperatures

Using the analyses of the previous sections, a calibration was made to determine fuel temperatures for steady state and pulse modes of operation. This section describes the calibration techniques.

A series of fuel temperature measurements were made using the 12 wt% U fuel instrumented fuel elements in core configuration loading 36 as shown in Figure 9-1. One instrumented fuel element, I-13, had been in the core since September 1977 (in the B ring, the position of MEPD) and the other, I-14, had never been used. The first series of measurements was taken with I-13 in the G-8 core position and I-14 in the G-10 core position. The core position of a fuel element is identified in Figure 9-1 by a letter for the vertical axis position and a number for the horizontal axis position. The instrumented fuel elements have been numbered sequentially with an I prefix. After rotating both fuel elements at 0.5 MW steady state operation to obtain maximum temperature readings, the reactor power was increased in steps to 0.7 MW, 0.9 MW, and 1 MW. The actual values of the power were 0.98 (for loading 36) of that read on the recorder because the readout on the linear recorder was adjusted to read 0.4 MW when the actual power, as determined by a thermal power calibration, was approximately 390 kW (see the description of C_1 immediately after Equation (15)).

After completing the series of steady state runs, the reactor was pulsed sequentially with 2, 2.25, 2.50, and 2.75 dollar pulses. Before each pulse, the reactor was made subcritical to allow the temperature to reach equilibrium.

The above experiment was then repeated to determine reproducibility and measure the effect of the gap in I-14 created by the 4 pulses. The above measurements were again repeated with I-13 positioned in G-10 and I-14 positioned in G-8 to again study the reproducibility of the data and obtain another measurement on the temperature drop across the fuel cladding gap, $\overline{\Delta t_g}$.

The steady state and pulse measurements were again repeated, first with I-14 in F-10 and then with I-14 in H-11; I-13 was in position in G-8 for both sets of these measurements.

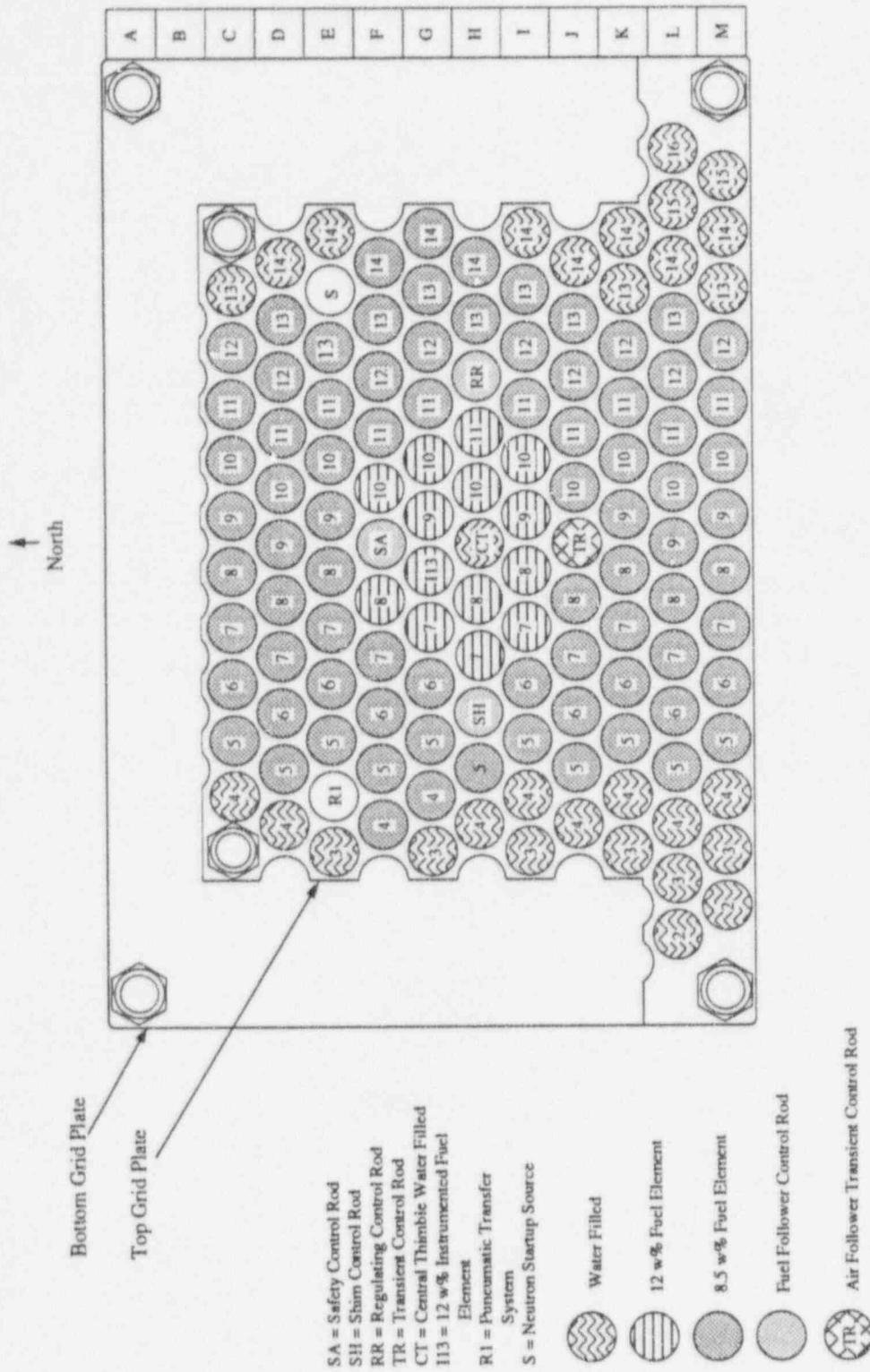


Figure 9-1 PSBR Core Configuration Loading 36

The data for all measurements (done prior to 1986) are summarized in Table 9-2. Both the chart recorder and the meter were used to measure the fuel temperature of I-13 as shown in Table 9-2. The chart recorder was connected to the thermocouple at the midplane of the fuel element, whereas, the meter was connected to the thermocouple located 1" below. The banked control rods during a pulse causes the position of the highest power density in the fuel element to be displaced slightly downward from the midplane of the fuel. This causes the meter readings to be approximately 24 °C higher than those read on the chart recorder.

4. Evaluation of $\overline{\Delta t_g}$ for Fuel Element I-14

The unused TRIGA 12 wt% U fuel instrumented fuel element, I-14, has been placed in the core configuration of Figure 9-1, Core Loading 36, and experiments performed to evaluate Equation (22). It is assumed that before pulsing the instrumented fuel element, I-14, it had a $\overline{\Delta t_g}$ equal to 0 as the fuel would be in contact with the cladding. When the fuel element is first pulsed, the cladding is stretched introducing a gap which increases the $\overline{\Delta t_g}$. After a number of pulses of the same size (i.e. \$2.50), $\overline{\Delta t_g}$ reaches a maximum value and does not increase with further pulsing.⁽⁴⁾

The increase in $\overline{\Delta t_g}$ after pulsing I-14 several times is now determined by comparing the steady state temperatures for the same condition after each set of pulses. It has been found that measured fuel temperatures will increase further due to an increase in $\overline{\Delta t_g}$ when at some later time pulses of a larger size are performed (i.e. \$3.00).^(25, 26)

At 1 MW, I-14 measured $t_{fc} = 372$ °C in Core Loading 36 and position G-10 before any pulsing began. (Note that for work that was done for the original SAR $C_f = 0.98$ and $f_a = 1.35$ and for subsequent analyses 1 and 1.25 are used respectively. The former because of the reasons stated immediately after Equation (15) and the latter because the 1.25 is a more typical value used as a design specification for axial peaking for TRIGA fuel (31)) Using Equation (22),

$$372 = 0.98 \frac{9.024 \times 10^3}{94.6} \times 1.35 NP_i + 140,$$

it follows that

$$NP_i = \frac{372 - 140}{128.8 \times 0.98} = 1.84.$$

After 4 pulses

$$t_{fc} = 418 \text{ °C},$$

and thus using Equation 22 again while holding NP_i constant at 1.84,

$$418 = 0.98(95.39 + \overline{\Delta t_g})(1.35)(1.84) + 140,$$

or

$$\overline{\Delta t_g} = 19 \text{ °C}.$$

Table 9-2

Fuel Temperature Measurement Data for Loading 36
 $T_o = 21^\circ\text{C}$

Fuel Element	Core Position	$t_{tc}(^\circ\text{C})$ SS 1 MW	$t_{po}(^\circ\text{C})$ Recorder/Meter			
			Pulse \$2.00	Pulse \$2.25	Pulse \$2.50	Pulse \$2.75
I-13	G-8	412	353/379	392/421	436/467	478/509
I-13	G-8	411	---	---	---	---
I-13	G-8	411	343/381	387/421	431/461	478/511
I-13	G-8	411	350/381	389/419	435/466	478/511
I-14	G-8	455	389	427	468	517
I-14	G-8	466	395	434	482	518
I-13	G-10	381	323/333	359/371	399/412	430/453
I-13	G-10	382	311/332	357/373	400/416	439/453
I-14	G-10	372	339	375	415	456
I-14	G-10	418	---	---	---	---
I-14	G-10	450	348	391	425	466
I-14	G-11	433	342	373	411	449

I-13 is a 12 wt% U fuel element burned to 2.2 Megawatt days

I-14 is a fresh 12 wt% U fuel element

These data and analysis show the initial (few pulses) increase in the temperature across the gap. Further data has shown that the increase in $\overline{\Delta t_g}$ diminishes to zero with successive pulses (see Table 9-2, lines 9 and 10). Element I-14 was then moved from position G-10 to position G-8 in the B-ring where the NP_i is different from that in G-10.

Assuming $\overline{\Delta t_g} = 19^\circ\text{C}$ and using $t_{ic} = 445^\circ\text{C}$ as measured in its new position at 1 MW, it follows that

$$445 = 0.98 (114.4) 1.35 NP_i + 140.$$

Therefore,

$$NP_i = 2.02.$$

After 8 pulses, the t_{ic} for element I-14 was measured again in position G-8. This time t_{ic} was 466°C at 1 MW. Therefore, using Equation (22) while holding NP_i constant at 2.02,

$$466 = (96.4 + \overline{\Delta t_g})(1.35)(2.02)0.98 + 140,$$

we find

$$\overline{\Delta t_g} = 26.6^\circ\text{C}.$$

It can be observed that after 8 pulses, $\overline{\Delta t_g} = 26.6^\circ\text{C}$. Past studies have shown that additional pulses do not alter the $\overline{\Delta t_g}$ significantly.⁽²⁵⁾ For I-14, it is assumed that after many more pulses of the same size (i.e. \$2.50), the $\overline{\Delta t_g}$ increase will be 1°C , hence we use

$$\overline{\Delta t_g} = 27.6^\circ\text{C},$$

and Equation (22) becomes for Loading 36 at $Q = 1$ MW

$$(t_{ic})_i = 163C_i NP_i + 140. \quad (32)$$

Equation (32) can now be used to determine the NP_i for I-14 anywhere in Core Loading 36 at 1 MW power as long as larger sized pulses are not performed resulting in an increase in $\overline{\Delta t_g}$.⁽²⁵⁾ To generalize Equation (32) for any core configuration and similar fuel element design specifications, it is only necessary to account for N_c . If this is done, Equation (32) becomes

$$(t_{ic})_i = \frac{1.57 \times 10^4}{N_c} C_i NP_i + 140. \quad (33)$$

The steady state data of Table 9-2 has been evaluated using Equation (33) and the results are tabulated in Table 9-3. The t_{ic} for the G-10 position was not measured after all pulsing had ceased and, therefore, is not listed in Table 9-3.

Table 9-3

Evaluation of NP_j 's from I-14 Data

Core Position	t_{ic} (°C)	NP_j Steady State Eq. (33)	NP_j (Ave) Pulse Eq. (34)
G-8	467	2.01	2.07
F-10	450	1.90	1.85
H-11	433	1.80	1.78
G-10		1.84	1.80

Table 9-4

Pulse Parameter Characteristics of Fuel Element I-14

Core Position	NP_j	M_j $\times 10^4$ °C/δk/k	M_j/NP_j $\times 10^4$ °C/δk/k	b_j °C	b_j/NP_j °C
G-10	1.84	2.23	1.21	162	88
G-8	2.01	2.44	1.21	197	98
G-8	2.01	2.34	1.17	210	104
F-10	1.90	2.25	1.18	170	89
H-11	1.80	2.04	1.13	178	99

Equation (33) is used to evaluate the measured fuel temperature during steady state operation. During steady state operation, the measured fuel temperature is close to the maximum fuel temperature (within 5%). In this case, the LSSS of 650 °C is extremely conservative because under steady state conditions, the maximum fuel temperature is no greater than 682 °C (650 °C + 5%) and thus, is well below the safety limit fuel temperature of 1150 °C. For loading 36, an upper limit for the measured maximum fuel temperature can be determined by setting $NP = 2.2$. Extensive calculations have been performed^(1, 2, 5, 7, 27) to study the maximum power distribution produced by different core configurations with fresh 12 wt% U fuel in the B-ring and the other core configurations containing a mixture of both 12 wt% U fuel and 8.5 wt% U fuel. Future maximum steady state measured fuel temperature will be below the 650 °C LSSS.

5. Evaluation of the Pulse Data for Fuel Element I-14

Each series of pulse data using I-14 is fitted to a straight line to determine M_i and b_i of Equation (30). Table 9-4 summarizes the results, wherein the data in the last column show that b_i/NP_i is constant within $\pm 8\%$ for the different core positions. The constants K_{14} and $\bar{\delta}t_{po}$ are determined to be 1.22 and 71 respectively using Equation (31). Substituting these values and those from Table 9-1 into Equation (29) the result is

$$t_{poi} = 1.177 \times 10^4 NP_i \delta k_p + 95.8 NP_i + T_o. \quad (34)$$

Equation (34) is now used to evaluate NP_i for the various core positions. The results are shown in Table 9-5 give consistent values for NP_i using different pulse magnitudes. This validates Equation (34). The value of NP_i as obtained from steady state Equation (33) is in good agreement with the corresponding value of NP_i obtained using the pulse Equation (34). The highest measured fuel temperatures in fuel element I-14 are compared to that using Equation (34) in Figure 9-2. It can be observed that the measured temperatures are in good agreement with Equation (34).

The Penn State in-core fuel management codes were employed to determine the power distribution and NP_i 's for Core Loading 36. In a recent Ph.D. thesis,⁽¹⁶⁾ the group constants of the individual fuel elements were evaluated as a function of their burnup using the SCRAM code. The SCRAM code provides a simple but reasonably accurate method of depleting the PSBR core as has occurred since December 1965. These constants were input into the EXTERMINATOR-2 code to obtain the NP_i 's for Core Loading 36. The NP_i 's for G-9 and H-10 with new 12 wt% U fuel varied between 2.03 and 2.10. This is to be compared with the measured values of 2.01 steady state and 2.07 by pulse. In general, the steady state and pulse NP 's agree with $\pm 3\%$.

It is now possible to eliminate the NP_i from Equation (32) and Equation (34) to give for I-14

$$t_{poi} - T_o = (72.28 \delta k_p + 0.588) \frac{t_{toi} - 140}{C_i} \text{ } ^\circ\text{C}. \quad (35)$$

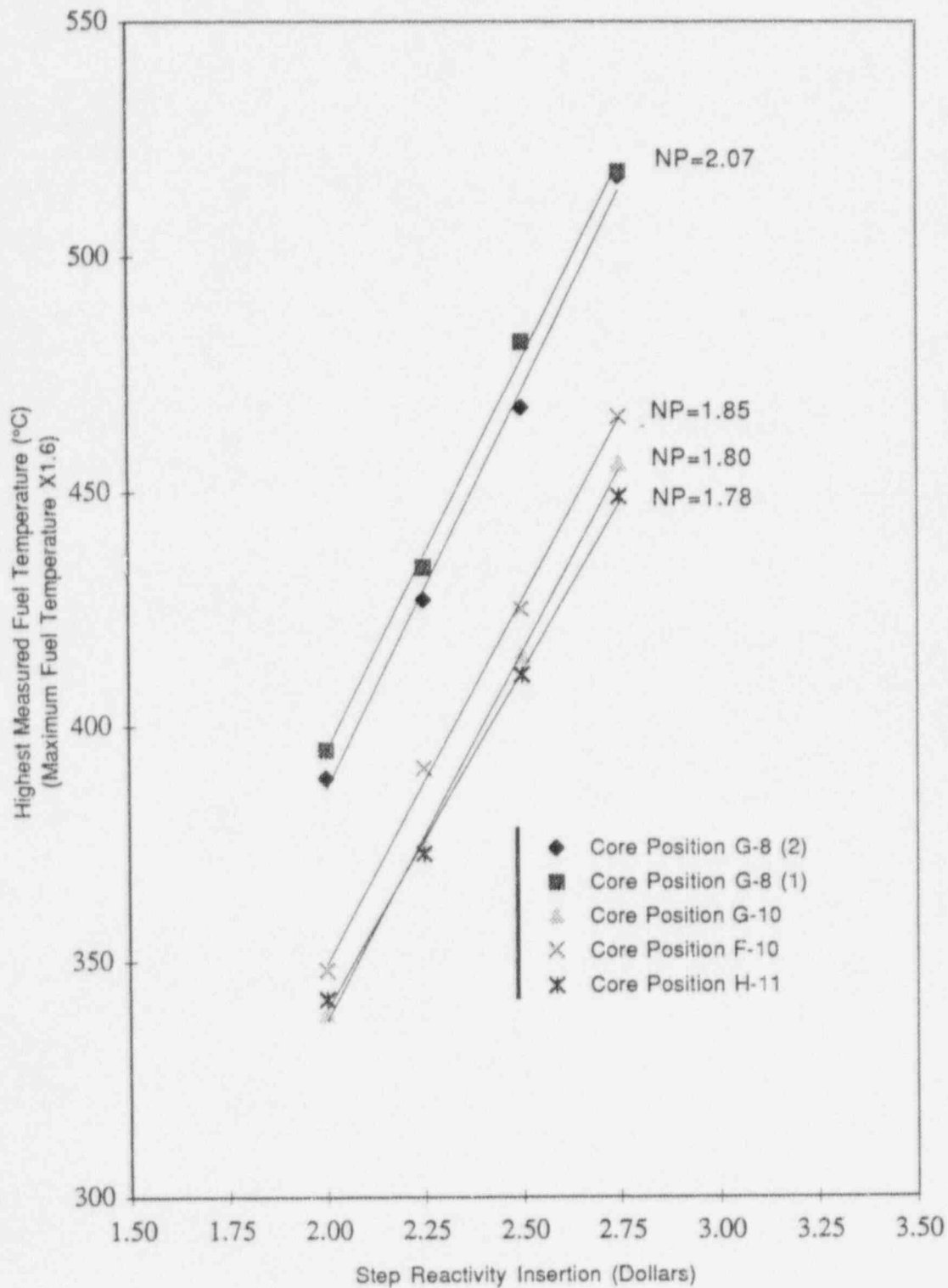


Figure 9-2. Comparing Highest Measured Fuel Temperatures During a Pulse With EQ(34) For Fuel Element I-14

January 14, 1997 Rev. 1 (4/24/97)

Equation (35) is an equation developed for fuel element I-14. It can be used anywhere in the core to predetermine the highest measured fuel temperature as a function of pulse prompt excess reactivity insertion (δk_p). It will require using the I-14 measured temperature when operating at 1 MW with I-14 in the same core position. For Core Loading 36 and using a maximum value of $NP = 2.2$ and corresponding $t_{ic} = 499$ °C, see Equation (32), the maximum value for t_{poj} is 684 °C for a pulse reactivity insertion of \$3.50 assuming $T_o = 21$ °C and $C_i = 1.0$. This corresponds to the maximum fuel temperature of 1095 °C which is below the safety limit of 1150 °C for fuel damage.

Thus, in the future, Equation (28) can be used to evaluate and predict t_{poj} . This requires placing I-14 in the hottest spot in the core and running at 1 MW to evaluate t_{ic} . Then starting with a \$2 pulse, verify Equation (28) and predict t_{poj} for the high values of δk_p . The t_{poj} related to a \$2 pulse will be more than 100 °C below t_{poj} for a \$2.75 pulse and even much lower than that for a \$3.50 pulse. Hence, these initial pulses will produce

maximum measured fuel temperatures well below 700 °C and allow determining the maximum fuel temperature attainable at the maximum allowable reactivity insertion pulses. A 700 °C fuel temperature measured by the thermocouple in a 12 wt% U fuel element corresponds to a maximum fuel temperature of 1120 °C. This is below the maximum allowed 1150 °C.

6. Evaluation of the Fuel Element I-13 Temperature Data (Pulse and Steady State)

Table 9-2 shows the temperature data taken for I-13 and I-14. As expected, a review of these data shows that the measured temperature of I-13 during 1 MW steady state operation, t_{ic} , is significantly lower than the t_{ic} of I-14 for the same core positions. On the other hand, the I-13 measured pulse temperature data is not significantly lower than that of I-14 for the corresponding conditions. This is because the A_o and B_o constants of Equation (14) are not the same for I-13 and I-14. The depletion of the outer rim of fuel in I-13 during burnup, in addition to the burnup of ^{235}U in all of the fuel element, lowers the self-shielding of thermal neutrons. As a result, the $q'''(r)$ distribution for I-13 is much flatter than that of I-14. Using Equation (4) for I-13, and setting

$$A_o = 0.9267$$

$$B_o = 40$$

yields the results of the I-13 data as shown in Table 9-6. The equivalent of Equation (33) and Equation (34) for I-13 are Equation (36) and Equation (37) respectively.

$$(t_{ic})_I = \frac{1.68 \times 10^4}{N_c} C_i NP_i + 140 \quad (36)$$

$$t_{poj} = 1.475 \times 10^4 NP_i \delta k_p + 80 NP_i + T_o. \quad (37)$$

Table 9-5

Table of NP_j Determined for I-14 Using Pulse Data in Eq. (34)

δk_{ex} Dollars	δk_p Dollars	Core Positions				
		G-10	G-8	G-8	F-10	H-11
2.00	1.00	1.79	2.06	2.10	1.84	1.80
2.25	1.25	1.79	2.04	2.08	1.86	1.78
2.50	1.50	1.79	2.04	2.10	1.85	1.78
2.75	1.75	1.81	2.07	2.07	1.86	1.78
Ave NP_j		1.80	2.05	2.09	1.85	1.78

It can be observed that the agreement between the pulse data and steady state data for determining NP_j is not as good as that for I-14. This is due to the approximations made in deriving Equations (33) and (34), namely,

- a. The $A_0 + B_0 r^2$ shape of $q'''(r)$ approximates the excess burnup of U-235 at the perimeter of the U-ZrH fuel in I-13.
- b. The $\overline{\Delta t_g}$ for I-13 is probably different from that of I-14.

However, temperatures measured by I-13 are consistent for the purposes of monitoring the core fuel temperatures.

7. Conclusion (Temperature Analysis)

A major conclusion of this section (based upon the present fuel specifications) is that an unused instrumented 12 wt% U fuel element can be calibrated and used to monitor the maximum fuel temperatures in the core. Once calibrated, the fuel element will only be used to measure maximum fuel temperatures in new core configurations. For steady state operations a measured fuel temperature of 650 °C results in a maximum fuel temperature well below 1150 °C. Under these conditions, the measured fuel temperature is close to the maximum fuel temperature. For pulse operation, a measured 700 °C fuel temperature corresponds to a maximum fuel temperature of 1120 °C which is below 1150 °C. The safety limit shall not be exceeded during pulse or steady state operation.

Once a fuel element has been depleted, its maximum steady state temperature decreases as long as the gap between the fuel and the cladding remains the same. As experience has shown, pulsing at higher levels will increase the fuel/cladding gap and the maximum steady state temperature may increase before it starts to decrease. The fuel temperatures measured during steady state operation with a depleted fuel element are related to the fuel temperature of a new fuel element by a simple ratio. Hence, this ratio can be used to assess the maximum fuel temperature during steady state in a new fuel element. The maximum fuel temperatures measured with a depleted fuel element during a pulse are close to that in a new fuel element. The preferential depletion of the periphery of the fuel element causes the power distribution and hence, the temperature distribution during a pulse, to be flatter than that of a new fuel element. Thus, the measured fuel temperature in a depleted fuel element corresponds to a lower maximum fuel temperature. It is also closer to the average fuel temperature. The core average fuel temperature rise for a given δk_p insertion is the same for all cores. The lower NP for a depleted fuel element accounts for its being closer to the average core fuel temperature.

Table 9-6

Evaluation of NP_j's from I-13 Data
I-13 (1.2 MWD Depleted)

Core Position	t_{tc} (°C)	NP _j Steady State Equation (36)	NP _j (Ave) Pulse Equation (37)
G-8	411	1.56	1.62
G-8	382	1.39	1.54

For comparison, see I-14 data in Table 9-3.

C. Evaluation of the Limiting Safety System Setting (LSSS)

The limiting safety system setting is a measured fuel temperature of 650 °C as defined in the Technical Specifications.

If the core power were at 1.15 MW (15% over power) steady state, the measured fuel temperature in the B-ring using extrapolated experimental data for, Figure 9-3, Core Loading 47^b with 95.5 elements would be 650 °C, (using the 12 wt% U fuel element, I-15, which had been pulsed at the \$3 level 20 times). The maximum temperature will be slightly higher, but the fuel temperature near the cladding will be approximately half this temperature. The extrapolated 650 °C fuel temperature is close to the maximum fuel temperature (within approximately 5%) due to the radial temperature distribution. A sudden insertion of reactivity with power at 1.15 MW, close to but less than \$1, into the core will initially increase the reactor power exponentially at a period faster than one second. Using a negative temperature coefficient of $1 \times 10^{-4} \delta k / k^{\circ}C$,^c the increase in average core fuel temperature is less than,

$$\frac{0.0078k/k}{1 \times 10^{-4} \delta k / k^{\circ}C} = 70^{\circ}C$$

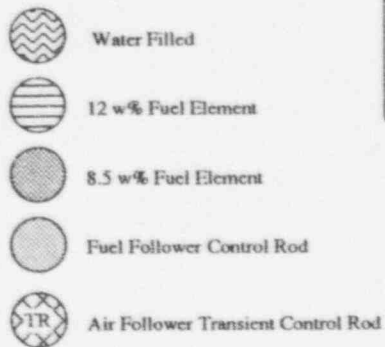
and for an NP = 2.2 and $f_a = 1.25$, the maximum fuel temperature increase is 193 °C ($2.2 \times 1.25 \times 70^{\circ}C = 193^{\circ}C$). Adding this increased fuel temperature in the hottest fuel element to the 650 °C steady state temperature results in 843 °C much less than the safety limit of 1150 °C. For this to occur at power levels above the power level scram setpoint will require that both power level scrams fail. The temperature scram will be initiated when the measured temperature exceeds its set point. The equilibrium temperature of 843 °C will be achieved at least within two to three periods (seconds) after reactivity insertion. A control rod drop time less than one second assures an early decrease in reactivity and fuel temperature. At this point, the control rods moving into the core will begin to decrease the reactor power in less than a second after the scram. Control rods are checked semiannually to assure their rod drop time is less than one second. The kinetics of the reactor cause the reactor power to decrease as soon as the control rods move a few inches into the core. Thus, the maximum fuel temperature will remain well below 1150 °C since the measured fuel temperature is close to the maximum fuel temperature for these quasi-static conditions.

The maximum allowed pulse reactivity of \$3.50 is established to prevent the fuel temperature from exceeding the safety limit of 1150 °C. A \$3.50 pulse, the maximum measured temperature starting from pool ambient temperature, using Equation (34) and

^b Core Loading 47 is considered an extrema loading relative to steady state measured peak fuel temperatures.

^c The temperature coefficient during a fast period is slightly less than the prompt temperature coefficient.

SA = Safety Control Rod
 SH = Shim Control Rod
 RR = Regulating Control Rod
 TR = Transient Control Rod
 CT = Central Thimble Water Filled
 I15 = 12 w% Instrumented Fuel
 Element
 R1 = Pneumatic Transfer
 System
 S = Neutron Startup Source
 PR = Power Range Gamma Ion
 Chamber
 WR2 = Wide Range Fission
 Chamber
 Chambers are located above
 the core



Bottom Grid Plate

Top Grid Plate

North

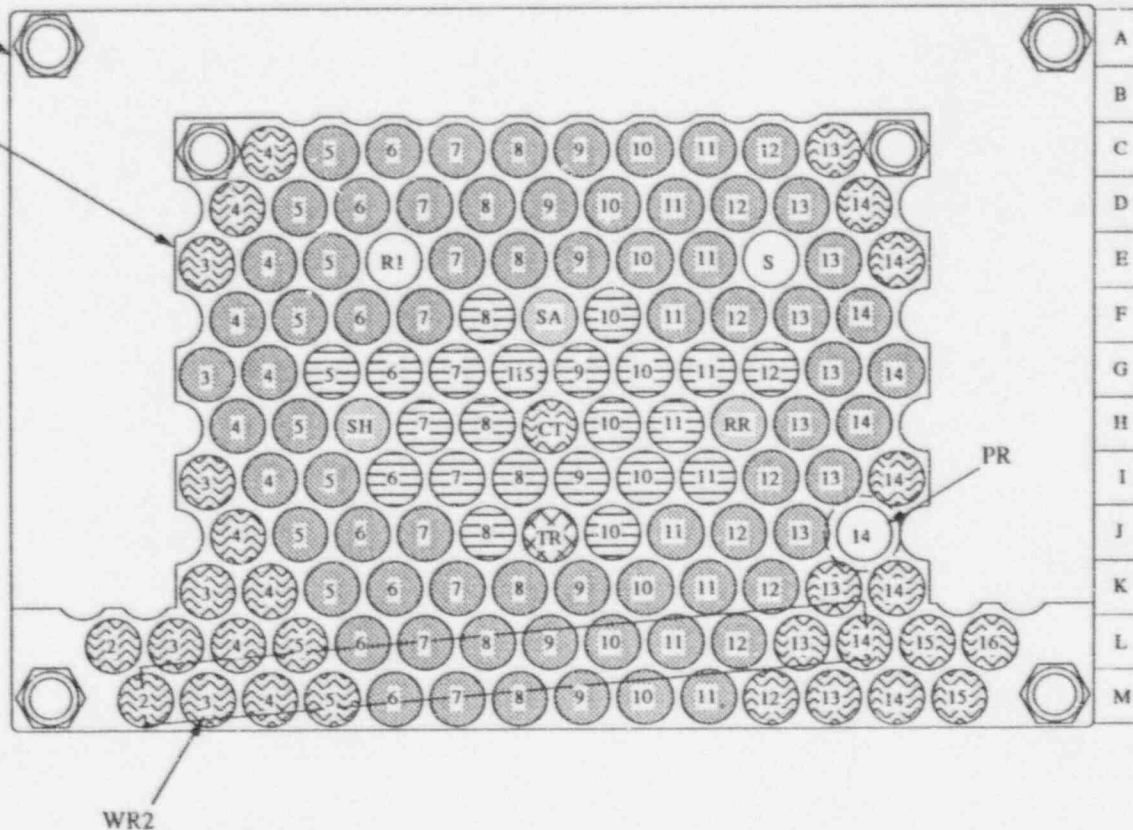


Figure 9-3 PSBR Core Configuration Loading 47

$NP = 2.2$, is 684°C . This corresponds to a maximum fuel temperature of 1095°C . The temperature scram will not lower the maximum fuel temperature attained during a pulse once the pulse is initiated; however, it does protect the core from high temperatures during steady state operation. The core average fuel temperature is independent of core size for a given δk_p insertion, therefore the maximum fuel temperature attained during a pulse for an $NP = 2.2$ is also independent of core size for a given δk_p insertion.

D. Loss of Coolant Accident

The PSBR pool contains 71,000 gallons of water. For a loss of coolant accident to occur, a break in the pool wall or break in a connecting pipe must occur below the bottom of the core. A series of alarms will occur as the water level drops more than 26 cm below reference pool full level. Just below 26 cm, alarms will notify the reactor operator in the control room and the University Police Services. If the reactor is operating at 1.0 MW, a low pool level alarm will alert the operator who is required by administratively approved procedure to shut down the reactor. There exists a moveable gate that can be used to isolate either side of the pool after the leak is noticed.

Emergency procedures call for moving the reactor to the non-leaking side of the pool and isolating that side of the pool with the gate to prevent the water level from dropping below the reactor core.

If the reactor is operating when the leak occurs the reactor operator will shut down the reactor upon receipt of the low pool level alarm. Within two minutes after the shut down the maximum fuel temperature will drop more than 350°C .⁽¹⁷⁾ Three minutes after the shut down the maximum fuel temperature is within 20°C of the water temperature.⁽¹⁷⁾

The largest conceivable LOCA is a break in the 6" pipe connected to the bottom of the pool. For this LOCA, it will take more than 1360 seconds (22.6 min.) before the water falls below the bottom of the reactor core. Therefore, the minimum time before air convection cooling occurs is about 23 minutes after a LOCA. The fuel has been within 20°C of the water temperature for approximately 20 minutes before air convection cooling begins.

As soon as the water falls below the reactor core, the fuel temperature will begin to rise, because the natural air convection cooling is less effective than water. The rate of rise of the fuel temperature will depend on the previous operating history of the reactor, and the effectiveness of natural air convection to cool the fuel elements. The time it takes for the water to fall below the bottom of the core once LOCA occurs is θ_s . The time it takes once air cooling begins until the fuel temperature reaches its maximum temperature is θ_e . Thus, the total time, t , starting when the LOCA occurs until the fuel reaches its maximum temperature, is the sum of two times θ_s and θ_e .

General Atomic conducted a set of LOCA experiments for TRIGA reactors.⁽¹⁸⁾ In these experiments dummy TRIGA fuel elements were electrically heated in a grid to determine the rate of temperature increase of TRIGA fuel elements when cooled by natural air convection. The dummy fuel elements were wound with resistance wire to simulate a cosine distribution similar to that produced in the core. The standard TRIGA grid-plate assembly pitch for a circular (non-hexagonal) core was used with a seven element assembly to mock-up the central portion of a standard core. The LOCA experiments were more conservative for two reasons.⁽¹⁾ The PSBR does not have a central fuel element in the core to block the air flow in the hottest part of the core.⁽²⁾ In addition, the hexagonal pitch of the PSBR is less likely to produce hot spots on the cladding. When the core is uncovered, the central part of the PSBR core will allow more efficient cooling of the fuel elements in the B-ring increasing the safety factor associated with these calculations.

The time θ_s may be computed assuming the 6" drain pipe at the bottom of the pool ruptures. In this case,

$$\theta_s = 1360 \text{ sec. (23 min.)}$$

To calculate the time θ_e , it is necessary to review GA's results as summarized in Figure 9-4 and 9-5. Figure 9-4 shows that with a constant cosine shape power input of 267 watts, it takes approximately $\theta_e = 300$ minutes before the maximum fuel temperature reaches the equilibrium temperature, T_{eqfuel} , of 600 °C. The maximum fuel temperature attainable, i.e., T_{eqfuel} as a function of the source power in watts, is given in Figure 9-5. The thermal time constant of the fuel after a LOCA is approximately the same for all values of decay power. Thus, it will take 300 minutes once air cooling begins before the fuel temperature reaches T_{eqfuel} . The fitted equation for T_{eqfuel} as a function of θ_e and T_{max} (which in the case of Figure 9-4 is 600 °C) is as follows:

$$T_{\text{eqfuel}} = T_{\text{max}} (-8.063 \times 10^{-3} + 2.193 \times 10^{-2}\theta_e - 2.263 \times 10^{-4}\theta_e^2 + 1.193 \times 10^{-6}\theta_e^3 - 3.031 \times 10^{-9}\theta_e^4 + 2.929 \times 10^{-12}\theta_e^5), 0 < \theta_e < 300 \text{ minutes.} \quad (37a)$$

Before the maximum fuel temperature reached during a LOCA is determined, the core operation history and maximum fuel element powers must be established. As shown in Figure 9-5, the maximum fuel temperature reached during a LOCA is directly related to the decay power and the decay power is a function of the pre-LOCA reactor operating history.

The following assumptions are conservative and are used to determine the decay power. The PSBR is licensed for a maximum steady state power of 1 MW and normally operates on a 40 hr/wk schedule. Even when the reactor operates on a two shift schedule for reactor operator instruction or for laboratory experiments, the average power per 40 hr week is much less than 1 MW. For the 15 years from 1967-81, the PSBR was operated an average of 15 MW hr/wk. For the 13 years from 1981-94, the PSBR was operated an average of less than 5.5 MW hr/wk. Assuming the PSBR operates for 40 hours at 1 MW during the week establishes an upper limit for its operation. However, to cover any future increase in operational activities, it will be assumed that the reactor is operated continuously for one week at 1 MW. With this assumption, the fission product decay power can be determined in the following manner.

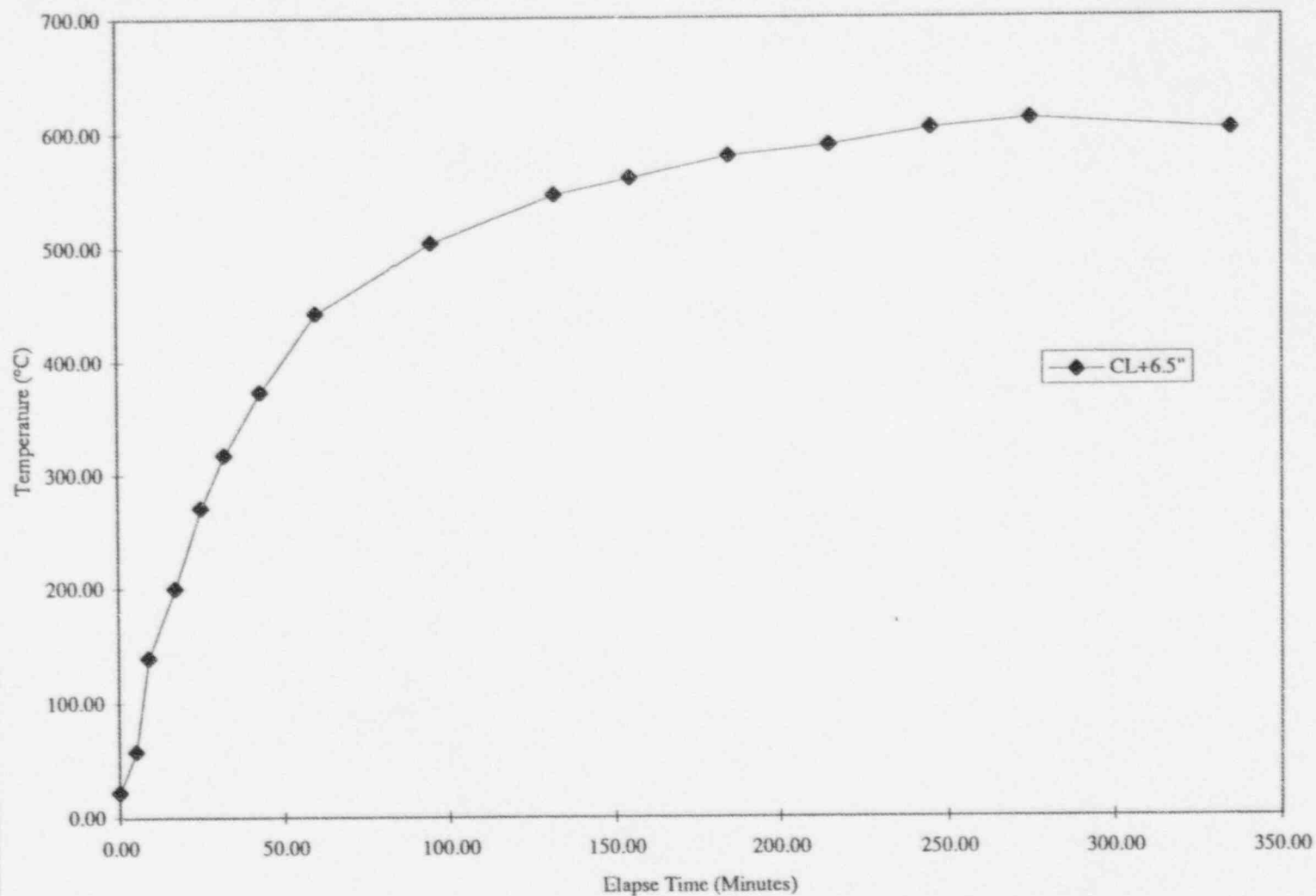


Figure 9-4 The Time Dependence of Air Cooled Fuel Body for Center Element With 267 W Input (Data from Reference 18)

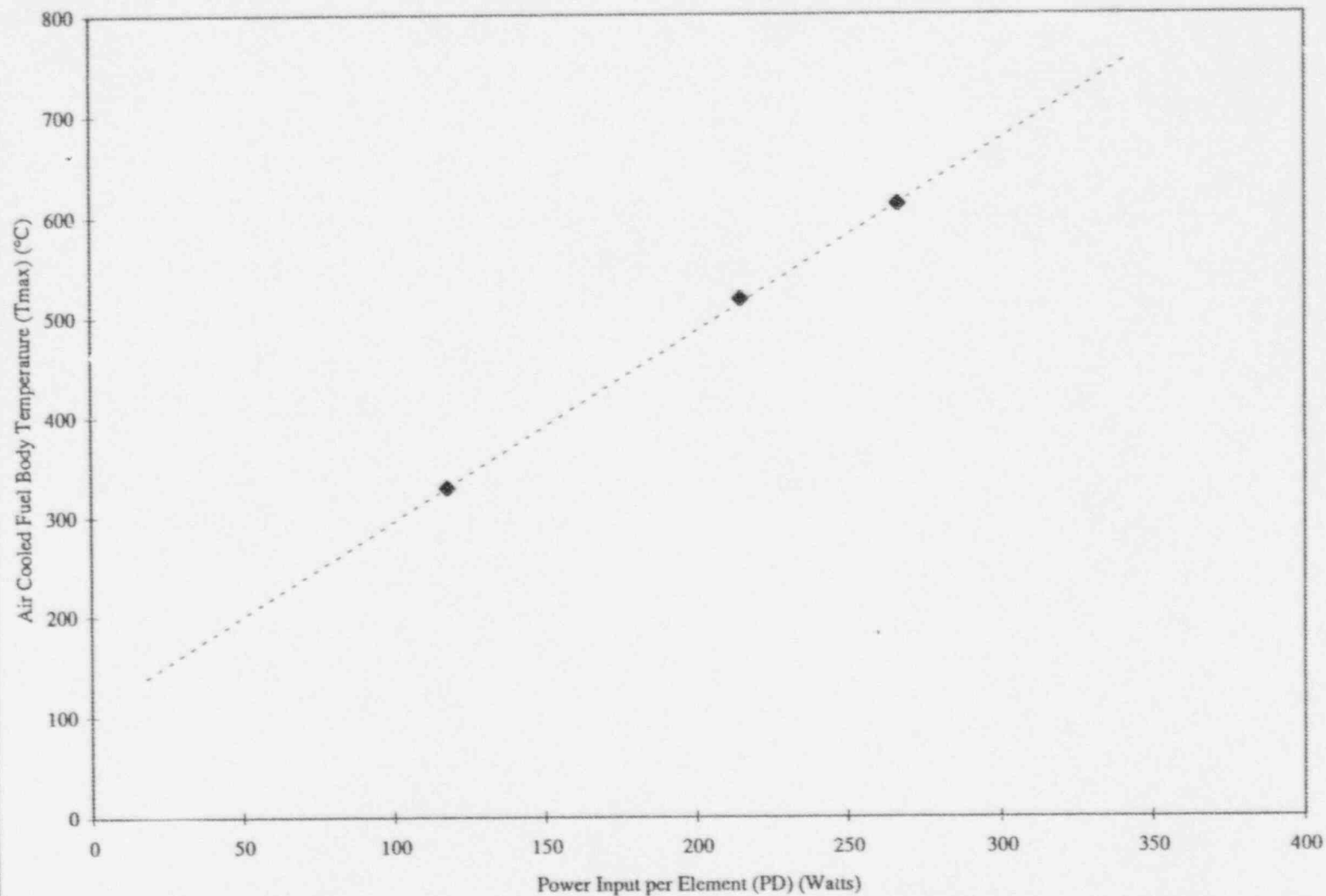


Figure 9-5 Summary of Equilibrium Data for LOCA Simulation Showing the Fuel Element Cladding Temperature versus Power Input to the Element for all Seven Dummy Elements Heated with the Same Power Input (Data from Reference 18).

El-Wakil⁽¹⁴⁾ gives the following equation for decay power:

$$\frac{P_s}{P_o} = \left[0.1(\theta_s + 10)^{-0.2} - 0.087(\theta_s + 2 \times 10^7)^{-0.2} \right] - \left[0.1(\theta_s + \theta_o + 10)^{-0.2} - 0.087(\theta_s + \theta_o + 2 \times 10^7)^{-0.2} \right] \quad (38)$$

where,

P_s = the power after shutdown produced by the fission product decay,

P_o = the steady state power before LOCA, i.e. 1 MW,

θ_s = the time after LOCA initiation, i.e., 1360 sec,

θ_o = the time of operation at power before LOCA, i.e.,
168 hr. \times 3600 sec/hr = 6.05×10^5 sec.

Using these values, at time θ_s after LOCA initiation or at the beginning of air convection cooling:

$$\frac{P_s}{P_o} = 1.65 \times 10^{-2},$$

or if we assume a maximum elemental power density, MEPD, of 24.7 kW, the maximum power due to fission product decay, P_D at time θ_s , is

$$\begin{aligned} P_D &= \frac{P_s N_p 1000 \text{ kW}}{P_o} \\ &= 1.7 \times 10^{-2} \times 24.7 \text{ kW/fuel element} \\ &= 410 \text{ watts} \end{aligned} \quad (38a)$$

Assuming the core is uncovered and reaches equilibrium fuel temperature 1360 sec (~ 23 min.) after a LOCA, the hottest fuel element in the core will have less than 410 watts of power which will continue to decay.

Figure 9-5 shows the equilibrium fuel cladding temperature as a function of fuel element power input. The data of Figure 9-5 have been fit with a straight line equation, i.e.,

$$T_{\max} = \frac{P_D + 62.89}{0.5498}, \quad (39)$$

where P_D is the decay power (watts) producing temperature in °C.

When $P_D = 410$ watts then $t_{\max} = 860$ °C.

This shows, that once air cooling begins and if the average decay power remains constant at 410 watts for approximately 4 hours the maximum fuel temperature is 860 °C. However, the decay power does not remain constant but decreases exponentially. By combining Equations (37a), (38), (38a), and (39) an equation of T_{eqfuel} as a function of time after the LOCA initiation is obtained. This equation indicates that the fuel reaches a maximum temperature of 468 °C approximately 7160 seconds after LOCA initiation, with a θ_s (drain down time) of 1360 seconds, and then continues to decrease (see Figure 9-6). If θ_s is reduced by half to 680 seconds the fuel reaches a maximum temperature of 480 °C approximately 6250 seconds after LOCA and then continues to decrease. For the most severely conceived LOCA for the PSBR, the maximum fuel temperature remains well below the 950 °C limit throughout the LOCA. It should also be stated that the experimental data of Figure 9-4 shows that because of the long time it takes to heat up a TRIGA fuel element, i.e. θ_e , once air cooling begins, the time θ_s is less critical.

The LOCA for a TRIGA core may also be analyzed analytically instead of by the results of experiments used above. General Atomic used one of their own two dimensional transient-heat transport computer codes to calculate the TRIGA fuel element temperature after the loss of pool water.⁽¹⁹⁾ It was assumed that the reactor was operating for an infinite period of time. Their results are plotted in Figure 9-7 for several cooling or delay times showing maximum fuel temperatures in the TRIGA fuel element as a function of its operating power. It can be observed that a fuel element having approximately 24.7 kW before the LOCA, will attain < 950 °C maximum temperature, 1360 seconds after the LOCA.

The 950 °C maximum fuel temperature is important when analyzing the TRIGA core for a LOCA. During a LOCA, the fuel element is uncovered producing cladding temperatures greater than 500 °C. Under these conditions, if 950 °C fuel temperature and 950 °C cladding temperature is reached or exceeded, the TRIGA cladding could be ruptured.^(13, 30) Below a fuel temperature of 950 °C the cladding remains intact. The strength of the fuel element cladding is a function of its temperature. The yield strength of the stainless steel cladding (assuming that the cladding design specifications of the TRIGA fuel elements do not change between procurements from the as-tested cladding) under LOCA conditions (heated in air), is shown in Figure 9-8. Also shown in Figure 9-8 is the cladding stress produced by any gas in the gap. This gas pressure consists of the hydrogen gas pressure plus the pressure of the volatile fission products plus the pressure of the trapped air. It can be observed that the cladding stress equals the cladding yield strength at approximately 950 °C. This is different from the safety limit (1150 °C) which is the case when the cladding is in water and cladding temperatures remain below 500 °C.

The following results are applicable to the PSBR experiencing a LOCA:

1. The maximum temperature that the PSBR TRIGA fuel element can have during a LOCA without damage to the cladding is 950 °C. As long as the 950 °C temperature limit is not exceeded, there will be no stress sufficient to rupture the cladding thereby allowing the escape of fission products.

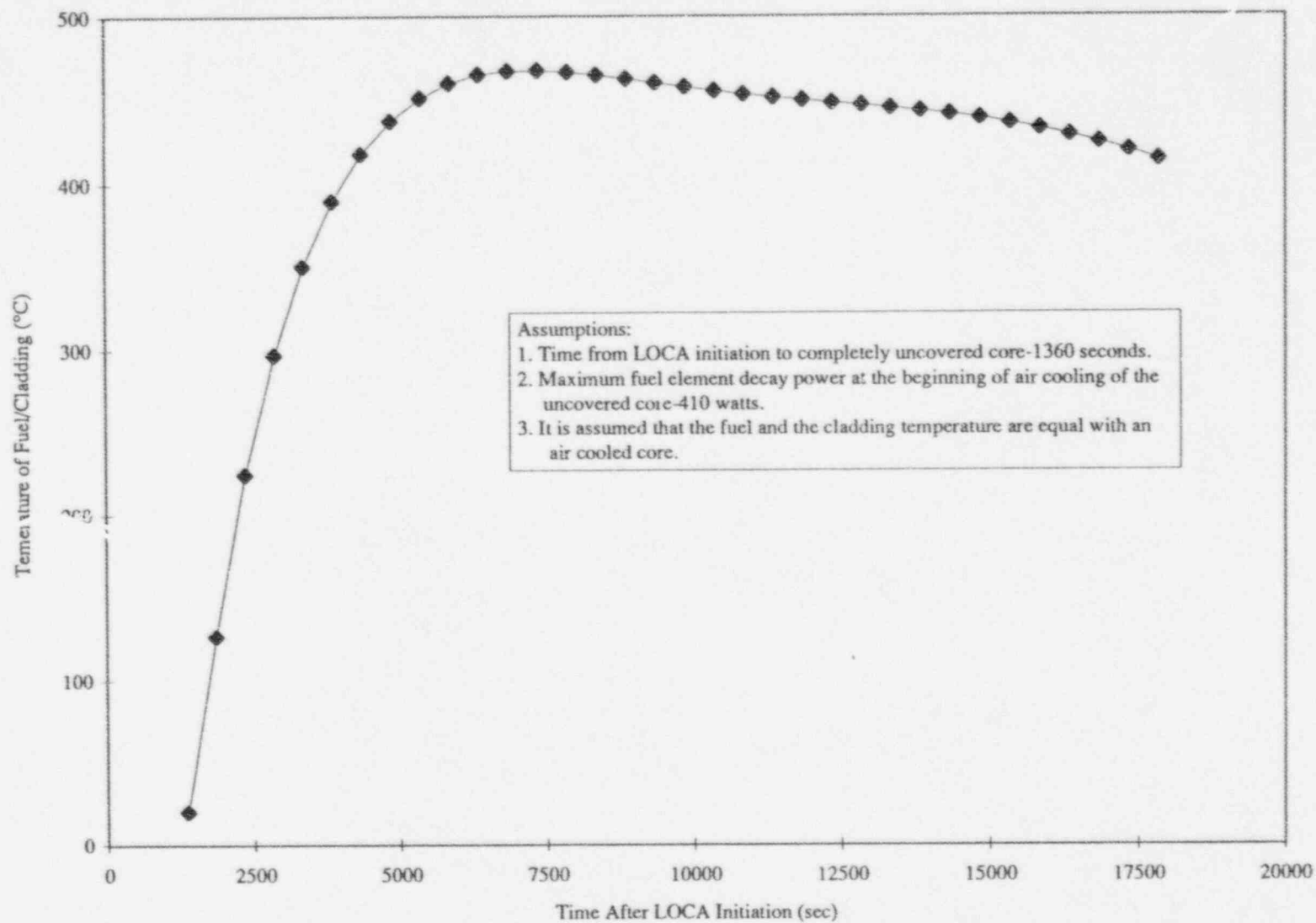


Figure 9-6 Fuel/Cladding Temperature as a Function of Time After LOCA Initiation

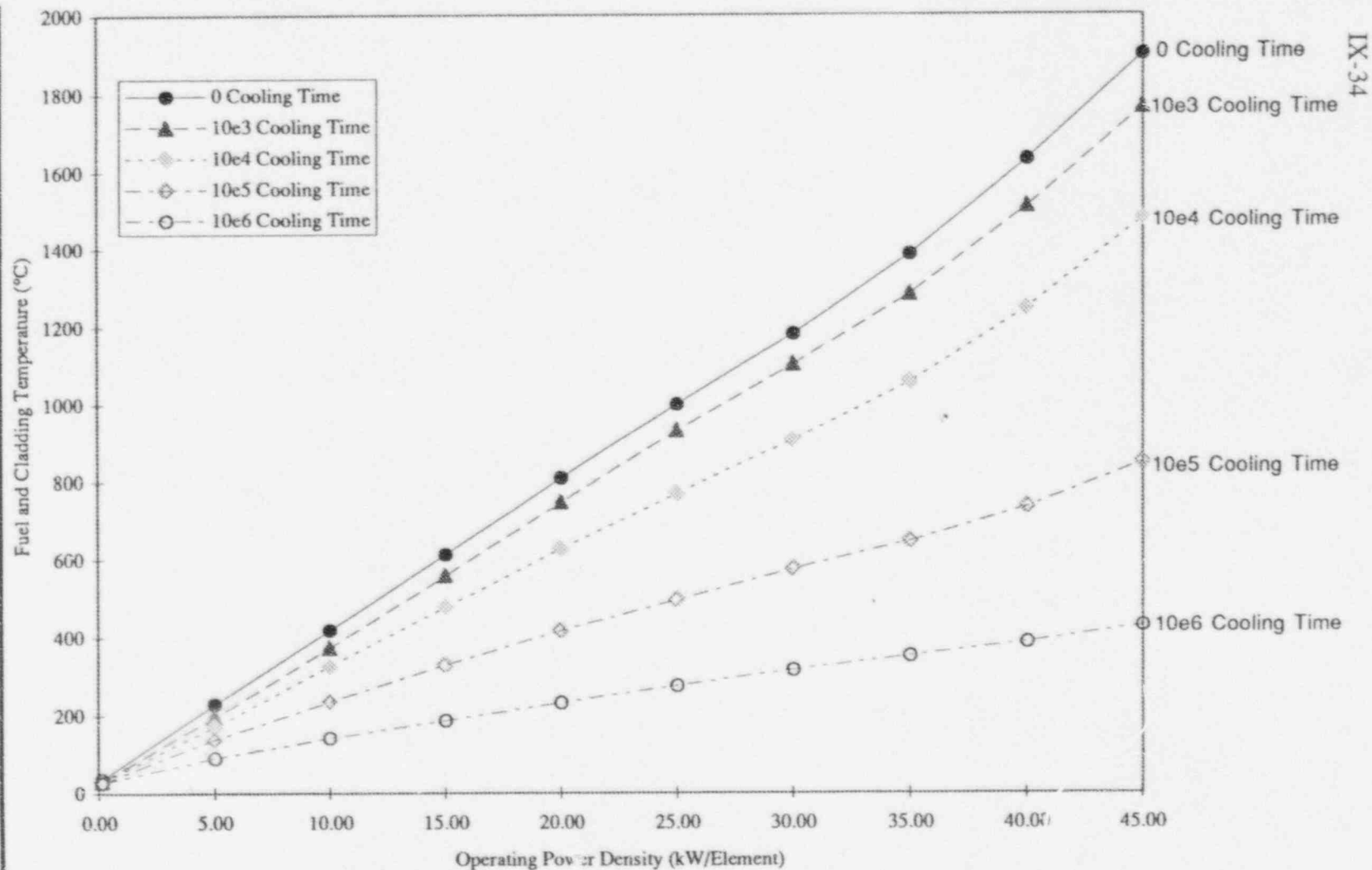


Figure 9-7 Maximum Fuel Temperature Versus Power Density After LOCA For Various Cooling Times Between Reactor Shutdown and LOCA Initiation (Data from Reference 19)

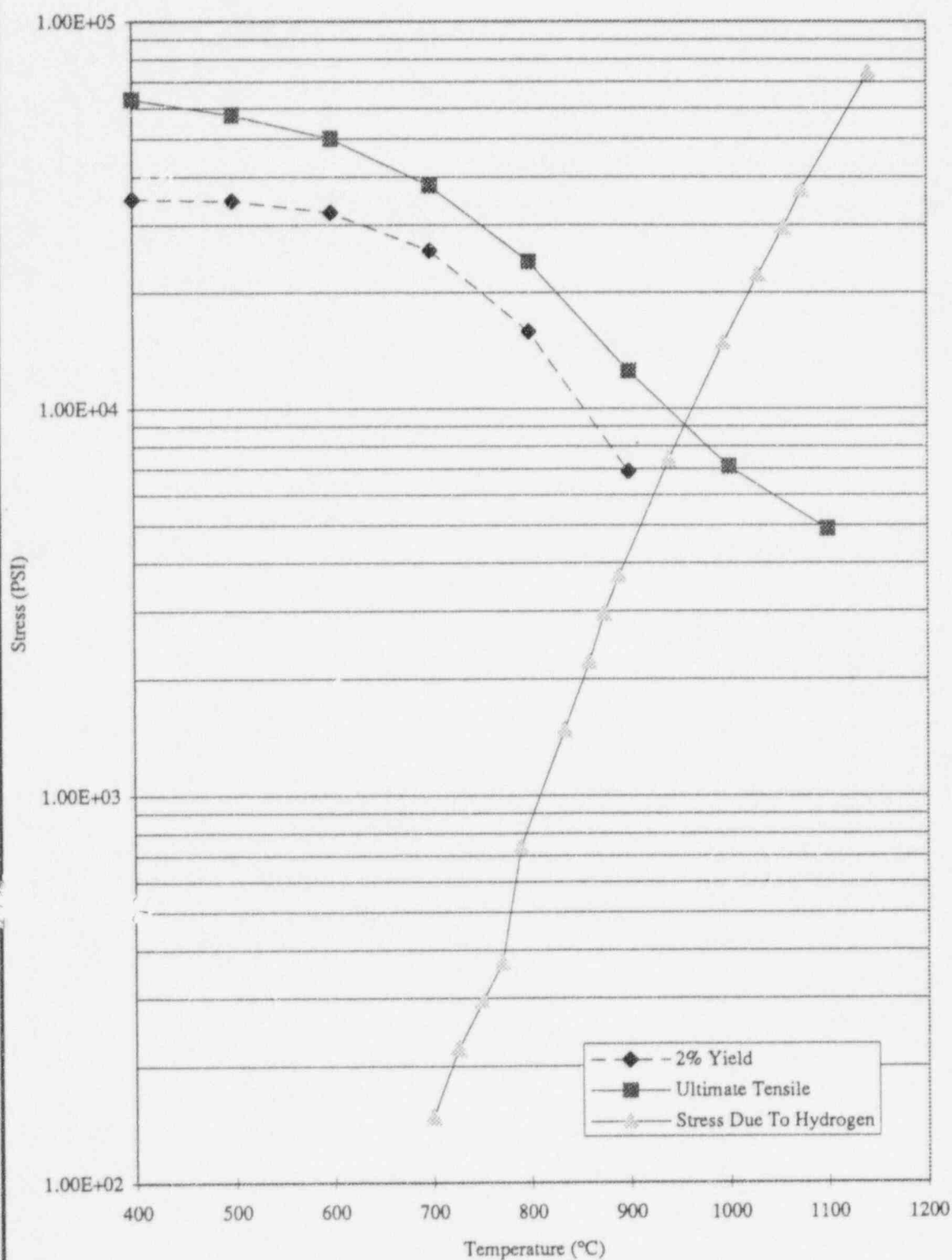


Figure 9-8 Strength and Applied Stress as a Function of Temperature, U-ZrH1.65 Fuel With Fuel and Cladding the Same Temperature (Data from Reference 13)

January 14, 1997 Rev. 1 (4/24/97)

2. Reviewing the complete history of the TRIGA cores at Penn State, the PSBR has never been operated for 40 hours at 1 MW during a week with the 12 wt% U fuel. In addition, no core configuration is permitted to operate at a power level such that the MEPD is greater than 24.7 kW. Assuming continuous operation at 1 MW with the 12 wt% U fuel producing 24.7 kW, a LOCA will not cause the fuel element to heat up to 950 °C under any condition.

In conclusion, a LOCA with the PSBR will not result in damaged fuel and, thus, fission product containment within the fuel is assured.

E. Maximum Hypothetical Accident (MHA)

The maximum hypothetical accident (MHA) is an assumption that a fuel element cladding ruptures in an air cooled core releasing volatile fission products to the reactor bay. The MHA is defined as a postulated accident with potential consequences greater than those from any event that can be mechanistically postulated. The assumptions create conditions far more severe than is actually possible. Nevertheless, the accident is bounded by the regulatory limits.

The potential hazards associated with the MHA are related to the escape of fission products from the ruptured cladding of a fuel element into the reactor bay and then from the bay to the environment. The fission product buildup in a fuel element is a function of the fuel element power history and sustained measured steady state fuel temperature. It is assumed in these calculations that the fuel element is a 12 wt% U-ZrH fuel element operated in the core position of highest power density. The core is assumed to operate continuously at 1 MW throughout its life. A review of the operating history of the 12 wt% U-ZrH fuel element I-15 shows that when operating at 1 MW it reached a maximum measured fuel temperature of ≈ 600 °C with Core Loading 47, however 650 °C is used as the bounding sustained measured steady state fuel temperature used to calculate the release fraction. Since all of the volatile fission products reach their maximum after a few weeks of operation, a value of MEPD = 24.7 kW is used to compute the fission product activity, A_{fp} , in a fuel element. It is assumed that the rupture occurs when the reactor is just completing continuous 1 MW operation. The saturated activity of the core, R , for one fission product (f_p) nuclide is

$$R = 1 \text{ MW} \times Y_D \frac{3.1 \times 10^{16}}{3.7 \times 10^{10}} \text{ curies} \quad (40a)$$

where,

$$\begin{aligned} Y_D &= \text{fission product cumulative yield} \\ 1 \text{ MW} &= 3.1 \times 10^{16} \text{ fission/sec} \\ 1 \text{ curie} &= 3.7 \times 10^{10} \text{ disintegration/sec} \end{aligned}$$

The fission product activity in the core is an accumulation of f_p activity from the previous weeks operation provided the half life is greater than approximately a day. The contribution to the f_p activity at the time of the rupture is as follows:

$R(1 - e^{-\lambda T_1})$	Activity produced during the week the rupture occurs,
$R(1 - e^{-\lambda T_1})e^{-\lambda(T_1 + T_2)}$	Activity produced during the week before the rupture occurs, and
$R(1 - e^{-\lambda T_1})e^{-\lambda n(T_1 + T_2)}$	Activity produced during the n^{th} week before the rupture occurs.

The total activity of this f_p in the core at the time of the rupture is the sum of the above activities. It can easily be shown that the core activity is

$$C_o = R \frac{1 - e^{-\lambda T_1}}{1 - e^{-\lambda(T_1 + T_2)}} \quad (40b)$$

and,

$$A_{fp} = \frac{NP}{N_c} R \frac{1 - e^{-\lambda T_1}}{1 - e^{-\lambda(T_1 + T_2)}} \quad (40c)$$

where in the case of continuous operation at 1 MW,

T_1	=	number of hours operated in one week = 168 hours
T_2	=	number of hours not operated in one week = 0 hours
$T_1 + T_2$	=	number of hours in one week = 168 hours

The PSBR presently operates on a 40 hr/wk schedule. The actual operation produces much less than 40 MWhr (MWhr) per week. For the 15 years from 1967-81, the PSBR operated an average of 15 MWhr/wk. For the 13 years from 1981-94, the PSBR was operated an average of less than 5.5 MWhr/wk. Continuous operation at 1 MW, therefore, establishes a large safety factor for this calculation, but allows for future increase of operating time.

Tables 9-7 and 9-8 lists the activity of each of the important gaseous fission products. The fission product yields were taken from the Katcoff, et.al., report.⁽²⁰⁾ These yields include direct production plus precursor decay from fission products. Only a fraction of these fission products escape from the fuel element into the reactor bay. The fraction that escapes from the fuel element is called the release fraction, f_r .

The fission product release fraction, determined experimentally at General Atomic, is a function of the sustained fuel temperature.⁽²¹⁾ The only fission products that escape are those that have diffused into the gap between the fuel and cladding during the operation of the reactor. Therefore, the release fraction in accident conditions is characteristic of the sustained normal operating temperature and not the temperature during an accident transient.

A review of the operating history of the instrumented fuel element I-13 in the PSBR B-ring shows that its maximum measured temperature during steady state operation at 1 MW was less than 460 °C. After the first year of operation, its measured temperature at 1 MW dropped to approximately 400 °C. During this period, its burnup was approximately 0.65 MWD. This temperature drop occurs because as burnup increases,

the ^{235}U core inventory decreases with a corresponding drop in NP and temperature. Operation after one year lowers the maximum measured fuel temperature in the B-ring to 400 °C or less. However, the experience mentioned above with I-15 in Core Loading 47, which is considered as an extreme (having a large peak to average temperature) core loading, indicates that measured fuel temperatures as high as 600 °C are possible. Thus, it is conservative to use a maximum measured fuel temperature of 650 °C, to compute the release fraction. Operation using the mixture of 12 and 8.5 wt% U fuel elements will only be allowed by Technical Specifications if the MEPD is ≤ 24.7 kW and the maximum measured fuel temperature, of an instrumented fuel element in the position of MEPD, is 650 °C. Thus the initial assumptions and the limits on operation resulting from this accident analysis are:

1. A maximum power operating history of continuous 1 MW operation.
2. A maximum sustained measured steady state fuel element temperature of 650 °C.
3. A MEPD of 24.7 kW.

Experiments demonstrated at General Atomic⁽²¹⁾ generated release fraction data for the U-ZrH fuel under various conditions. Below 400 °C the release fraction, f_r , is a constant, 1.5×10^{-5} , and above 400 °C the following equation is used:

$$f_r = 1.5 \times 10^{-5} + 3.6 \times 10^{-3} \exp\left(\frac{-1.34 \times 10^4}{T_o}\right) \quad (41)$$

where,

T_o is the fuel temperature in Kelvin.

For low temperature results, i.e., below 400 °C, the release fraction for a typical U-ZrH_x fuel element is constant, independent of operating history or details of operating temperatures. Averaging Equation (41) over the volume and temperature profile of the fuel element gives a release fraction of 3.1×10^{-4} using maximum measured fuel temperature of 650 °C. Applying the release fraction of 3.1×10^{-4} to a single element operating at a MEPD of 24.7 kW yields, for each fission product activity in Table 9-7 and 9-8, a release to the reactor bay of C_o curies. The bay concentration, C_b (Ci/ml) is based on a minimum free air bay volume of 1900 m³. An immediate and complete mixing is assumed to occur.

The concentration in the unrestricted area (outside the reactor building) is obtained by dividing the activity release rate through the emergency exhaust system by the dilution rate. The release rate for the emergency exhaust system is equal to the flow rate (3100 cfm or 1.46×10^6 ml/sec) times the bay concentration C_b . The dilution rate is the wind velocity (1 m/s) times the cross-section area of the building (200 m²) or 2×10^8 ml/sec. Thus, at the instant the fuel element cladding ruptures, the maximum concentration in the unrestricted area, C_u (Ci/ml) is:

$$C_u = C_b \times 7.30 \times 10^{-3} \text{ Ci/ml.}$$

Isotope	YIELD %	Half-Life Seconds	ACTIVITY, Ci			REACTOR BAY			UNRESTRICTED AREA		PERCENT OF ANNUAL LIMIT		
			CORE TOTAL (Ci)	MAXIMUM ELEMENT	Decayed Activity (Ci)	μCi/ml	DAC	FRACTION	LIMIT	Fraction	1 MIN	1 HOUR	24 HOURS
Kr-83m	0.5440	6.70E+03	4.56E+03	1.13E+02	1.13E+02	1.84E-05	1.00E-02	1.84E-03	5.00E-05	2.69E-03	1.49E-06	9.33E-06	9.75E-06
Kr-85m	1.0100	1.61E+04	8.46E+03	2.09E+02	2.09E+02	3.41E-05	2.00E-05	1.71E+00	1.00E-07	2.49E+00	1.39E-03	9.21E-03	9.73E-03
Kr-85	0.2930	3.38E+08	2.43E+03	6.06E+01	6.06E+01	9.89E-06	1.00E-04	9.89E-02	7.00E-07	1.03E-01	8.06E-05	3.99E-04	4.26E-04
Kr-87	2.7600	4.56E+03	2.31E+04	5.71E+02	5.71E+02	9.32E-05	5.00E-06	1.86E+01	2.00E-08	3.41E+01	1.51E-02	1.13E-01	1.17E-01
Kr-88	4.3900	1.02E+04	3.67E+04	9.06E+02	9.06E+02	1.48E-04	2.00E-06	7.39E+01	9.00E-09	1.20E+02	6.01E-02	4.33E-01	4.55E-01
Kr-89*	5.4700	1.89E+02	4.58E+04	1.13E+03	1.13E+03	1.85E-04	1.00E-07	1.85E+03	1.00E-09	1.35E+03	1.35E+00	9.65E-01	9.65E-01
Kr-90*	5.0000	3.23E+01	4.19E+04	1.03E+03	1.03E+03	1.69E-04	1.00E-07	1.69E+03	1.00E-09	1.23E+03	7.77E-01	1.76E-01	1.76E-01
Kr-91*	3.4500	8.80E+00	2.89E+04	7.14E+02	7.14E+02	1.16E-04	1.00E-07	1.16E+03	1.00E-09	8.52E+02	2.02E-01	3.40E-02	3.40E-02
Kr-92*	1.8700	1.84E+00	1.57E+04	3.87E+02	3.87E+02	6.31E-05	1.00E-07	6.31E+02	1.00E-09	4.62E+02	2.32E-02	3.88E-03	3.88E-03
Kr-93*	0.4900	1.28E+02	4.02E+03	9.93E+01	9.93E+01	1.62E-05	1.00E-07	1.62E+02	1.00E-09	1.18E+02	1.13E-01	6.08E-02	6.08E-02
Kr-94*	0.1000	2.10E-01	8.38E+02	2.07E+01	2.07E+01	3.38E-06	1.00E-07	3.38E+01	1.00E-09	2.47E+01	1.42E-04	2.37E-05	2.37E-05
Kr-95*	0.0070	7.80E-01	5.88E+01	1.45E+00	1.45E+00	2.36E-07	1.00E-07	2.36E+00	1.00E-09	1.73E+00	3.69E-05	6.16E-06	6.16E-06
KRYPTON TOTAL													
Xe-133m	0.1600	1.89E+05	1.34E+03	3.31E+01	3.31E+01	5.40E-06	1.00E-04	5.40E-02	6.00E-07	6.58E-02	4.40E-05	2.53E-04	2.70E-04
Xe-133	6.6200	4.54E+05	5.55E+04	1.37E+03	1.37E+03	2.24E-04	1.00E-04	2.24E+00	5.00E-07	3.27E+00	1.82E-03	1.26E-02	1.34E-02
Xe-135m	1.8300	9.18E+02	1.53E+04	3.79E+02	3.79E+02	6.18E-05	9.00E-06	6.87E+00	4.00E-08	1.13E+01	5.47E-03	2.34E-02	2.35E-02
Xe-135	6.3000	3.27E+04	5.28E+04	1.30E+03	1.30E+03	2.13E-04	1.00E-05	2.13E+01	7.00E-08	2.22E+01	1.73E-02	8.39E-02	8.91E-02
Xe-137*	6.1700	2.31E+02	5.17E+04	1.28E+03	1.28E+03	2.08E-04	1.00E-07	2.08E+03	1.00E-09	1.52E+03	1.55E+00	1.28E+00	1.29E+00
Xe-138	5.4900	8.52E+02	4.60E+04	1.14E+03	1.14E+03	1.85E-04	4.00E-06	4.63E+01	2.00E-08	6.78E+01	3.68E-02	1.35E-01	1.36E-01
Xe-139*	5.4000	4.00E+01	4.52E+04	1.12E+03	1.12E+03	1.82E-04	1.00E-07	1.82E+03	1.00E-09	1.33E+03	9.27E-01	2.34E-01	2.34E-01
Xe-140*	3.8000	1.37E+01	3.18E+04	7.86E+02	7.86E+02	1.28E-04	1.00E-07	1.28E+03	1.00E-09	9.38E+02	3.31E-01	5.79E-02	5.79E-02
Xe-141*	1.3300	1.72E+00	1.11E+04	2.75E+02	2.75E+02	4.49E-05	1.00E-07	4.49E+02	1.00E-09	3.28E+02	1.55E-02	2.58E-03	2.58E-03
Xe-142*	0.3500	1.22E+00	2.99E+03	7.24E+01	7.24E+01	1.18E-05	1.00E-07	1.18E+02	1.00E-09	8.64E+01	2.89E-03	4.82E-04	4.82E-04
Xe-143*	0.0510	9.60E-01	4.27E+02	1.06E+01	1.06E+01	1.72E-06	1.00E-07	1.72E+01	1.00E-09	1.26E+01	3.31E-04	5.52E-05	5.52E-05
Xe-144*	0.0060	1.10E+00	5.03E+01	1.24E+00	1.24E+00	2.03E-07	1.00E-07	2.03E+00	1.00E-09	1.48E+00	4.46E-05	7.45E-06	7.45E-06
XENON TOTAL													
												2.9	1.8
												8.53E+03	3.6
												5.4	3.7

Table 9-7 Fission Product Data and Fission Product Release for the Noble Gases
For notes see table 9-8

Isotope	YIELD %	Half-Life Seconds	ACTIVITY, Ci			REACTOR BAY			UNRESTRICTED AREA		PERCENT OF ANNUAL LIMIT		
			CORE TOTAL (Ci)	MAXIMUM ELEMENT	Decayed Activity (Ci)	$\mu\text{Ci/ml}$	DAC	FRACTION	LIMIT	Fraction	BAY		UnRestricted Area
											1 MIN	1 HOUR	24 HOURS
Br-83	0.5100	8.64E+03	4.27E+03	1.06E+02	1.06E+02	1.72E-05	3.00E-05	5.74E-01	9.00E-08	1.40E+00	4.66E-04	4.97E-03	5.22E-03
Br-84	0.0190	3.60E+02	1.59E+02	3.93E+00	3.93E+00	6.42E-07	2.00E-05	3.21E-02	8.00E-08	5.86E-02	2.47E-05	6.90E-05	6.90E-05
Br-84m*	0.9200	1.91E+03	7.71E+03	1.90E+02	1.90E+02	3.11E-05	1.00E-07	3.11E+02	1.00E-09	2.27E+02	2.50E-01	6.25E-01	6.36E-01
Br-85*	1.1000	1.72E+02	9.22E+03	2.28E+02	2.28E+02	3.71E-05	1.00E-07	3.71E+02	1.00E-09	2.72E+02	2.69E-01	1.80E-01	1.80E-01
Br-87*	2.0000	5.61E+01	1.68E+04	4.14E+02	4.14E+02	6.75E-05	1.00E-07	6.75E+02	1.00E-09	4.94E+02	3.89E-01	1.19E-01	1.19E-01
Br-88*	3.8400	1.64E+01	3.22E+04	7.95E+02	7.95E+02	1.30E-04	1.00E-07	1.30E+03	1.00E-09	9.48E+02	3.87E-01	6.99E-02	6.99E-02
Br-89*	5.4000	4.40E+00	4.52E+04	1.12E+03	1.12E+03	1.82E-04	1.00E-07	1.82E+03	1.00E-09	1.33E+03	1.60E-01	2.67E-02	2.67E-02
Br-90*	5.8800	1.80E+00	4.93E+04	1.22E+03	1.22E+03	1.99E-04	1.00E-07	1.99E+03	1.00E-09	1.45E+03	7.15E-02	1.19E-02	1.19E-02
BROMINE TOTAL			1.65E+05	4.07E+03	4.07E+03			6.46E+03		4.73E+03	1.5	1.0	1.0
I-129	0.8000	5.02E+14	6.70E+03	1.66E+02	1.66E+02	2.70E-05	4.00E-09	6.75E+03	4.00E-11	4.94E+03	5.50E+00	1.91E+01	2.03E+01
I-131	3.1000	6.95E+05	2.60E+04	6.42E+02	6.42E+02	1.05E-04	2.00E-08	5.23E+03	2.00E-10	3.83E+03	4.26E+00	1.48E+01	1.57E+01
I-132	4.3800	6.24E+03	3.67E+04	9.06E+02	9.06E+02	1.48E-04	3.00E-06	4.93E+01	2.00E-08	5.41E+01	4.00E-02	1.92E-01	2.01E-01
I-133*	6.9000	7.49E+04	5.78E+04	1.43E+03	1.43E+03	2.33E-04	1.00E-07	2.33E+03	1.00E-09	1.70E+03	1.90E+00	6.51E+00	6.93E+00
I-134	7.8000	3.16E+03	6.54E+04	1.61E+03	1.61E+03	2.63E-04	2.00E-05	1.32E+01	6.00E-08	3.21E+01	1.07E-02	1.00E-01	1.03E-01
I-135	6.1000	2.37E+04	5.11E+04	1.26E+03	1.26E+03	2.06E-04	7.00E-07	2.94E+02	6.00E-09	2.51E+02	2.39E-01	9.40E-01	9.96E-01
I-136*	3.1000	8.50E+01	2.60E+04	6.42E+02	6.42E+02	1.05E-04	1.00E-07	1.05E+03	1.00E-09	7.65E+02	6.75E-01	2.72E-01	2.72E-01
I-137*	6.2500	2.45E+01	5.24E+04	1.29E+03	1.29E+03	2.11E-04	1.00E-07	2.11E+03	1.00E-09	1.54E+03	8.32E-01	1.68E-01	1.68E-01
I-138*	5.6600	6.50E+00	4.74E+04	1.17E+03	1.17E+03	1.91E-04	1.00E-07	1.91E+03	1.00E-09	1.40E+03	2.47E-01	4.13E-02	4.13E-02
I-139*	5.6300	2.40E+00	4.72E+04	1.17E+03	1.17E+03	1.90E-04	1.00E-07	1.90E+03	1.00E-09	1.39E+03	9.12E-02	1.52E-02	1.52E-02
IODINE TOTAL			4.17E+05	1.03E+04	1.03E+04			2.16E+04		1.59E+04	14	42	45
HALOGEN TOTAL			5.81E+05	1.44E+04	1.44E+04			2.81E+04		2.06E+04	15	43	46
NOBLE GAS PLUS HALOGEN			1.11E+06	2.74E+04	2.74E+04			3.96E+04		2.92E+04	21	47	50
Approximate TEDE =											1038	24	26
Approximate Thyroid Dose =											6415	698	744

Table 9-8 Fission Product Data, Fission Product Release for the Halogens and the Restricted and Unrestricted TEDE for the MHA

TABLE 9-7, 8 NOTES

COOL DOWN TIME	0.00 hr
RELEASE FRACTION	3.10E-04
BAY VOLUME	1.90E+09 ml
EXHAUST VENTILATION	1.46E+06 ml/sec
BUILDING DILUTION	2.00E+08 ml/sec
NUMBER OF FUEL ELEMENTS	100

IRRADIATION TIME TO MAXIMIZE ACTIVITY $\text{Core activity} = R \cdot \text{yield} [1 - e^{-(\lambda \text{bda} \cdot T_1)}] [1 - e^{-(\lambda \text{bda} (T_1 + T_2))}]$

P= 1	MW power level
T1= 168	hr/wk operating time
T2= 0	hr/wk shutdown
R= 3.1E+18	fissions/sec at 1 MW
NP= 2.47	ratio of maximum to average fuel element activity

* A DAC value of 1E-7 is used for those radioisotopes with half-life <2 hours and not listed in 10CFR20 Appendix B.

* A concentration limit of 1E-9 is used for unrestricted areas for those radioisotopes with half-life <2 hours, which are not listed in 10CFR20 Appendix B.

Percent of annual limit is based on 2000 DAC-hours for the reactor bay and 8760 "limit-hours" for the unrestricted area.

Thyroid Dose includes percent of annual limit for submersion and internal dose from I-129 through I-135.

Annual thyroid dose limit is estimated from a 50,000 mrem limit for restricted areas and 1670 mrem for unrestricted areas (50 mrem CEDE/0.03 tissue weighting factor).

In the reactor bay (restricted area), the concentration in air of airborne activity decreases with time because of radioactive decay and the removal of air by the emergency exhaust system.

Consider a model in which activity, released from the single fuel element, instantly mixes completely with air in the bay. The resulting uniform concentration is C_b . We have, then,

$$C_T = C_b e^{-(\lambda_d + \lambda_r)T} \quad (42)$$

where,

$$\begin{aligned} C_T &= \text{bay air concentration of activity at elapsed time } t \text{ after release from} \\ &\quad \text{the single fuel element (Ci/ml)} \\ \lambda_d &= \text{decay constant (sec}^{-1}\text{)} \\ \lambda_r &= \text{ventilation rate constant (sec}^{-1}\text{)} \\ \lambda_r &= \frac{\text{ventilation rate}}{\text{bay volume}} = \frac{1.46 \text{ m}^3 \text{ sec}^{-1}}{1900 \text{ m}^3} = 7.7 \times 10^{-4} \text{ sec}^{-1}. \end{aligned}$$

The exposure to an airborne concentration is equal to the integral of C_T over the period T , labeled IC_T .

$$IC_T = \frac{C_b}{\lambda_d + \lambda_r} \left(1 - e^{-(\lambda_d + \lambda_r)T} \right). \quad (43)$$

The reactor bay exposure in DAC-hours (derived air concentration hours) is equal to IC_T divided by the DAC value from 10 CFR Part 20 Appendix B. The same technique is used to determine the exposure in effluent limit concentration hours for the unrestricted area. The exposures determined for the reactor bay and the unrestricted area are then compared to the limits of 2000 DAC-hours for the reactor bay and 8760 effluent limit concentration hours for the unrestricted area, respectively, to arrive at the percent of the annual limit.

The activity is removed rapidly from the reactor bay and about 92% of the TEDE in the unrestricted area is received in the first hour. Essentially all activity has been released to the unrestricted area within 24 hours and doses in both the reactor bay and the unrestricted area have reached their maximum values. Release of the activity from a fuel element over an extended period of time would reduce the dose because of the decay of short half-life radioisotopes before release.

The total exposure in 1 minute for the reactor bay (1 minute is considered a maximum evacuation time) is a TEDE of about 1038 mrem, corresponding to about 21% of the annual 10 CFR Part 20 limit. An exposure time of 7.5 minutes in the reactor bay would be required to reach a TEDE of about 4988 mrem, corresponding to about 99% of the annual 10 CFR Part 20 limit.

The total exposure in the unrestricted area is about 26% of the annual limit, which corresponds to a TEDE in 24 hours of about 26 mrem (the annual limit in the unrestricted area is 50 to 100 mrem depending on the fractions of the dose from radioisotopes with an internal dose component).

Since the emergency exhaust system removes the bay air through a charcoal filter, the iodine exposure in the unrestricted area should be less than 10% of that given in Table 9.7. Since credit is not taken for the emergency exhaust system filtration in determination of the consequences of this accident, a Technical Specification requiring filtration as a limiting condition for operation is not required.

The above calculations assumed an MEPD of 24.7 kW and a maximum measured fuel temperature of 650 °C. Using the higher temperature increases the release fraction and the higher power density increases the fission product inventory. In addition, it was assumed that there are no mitigating circumstances such as fission products plating out on surfaces or dissolving in the pool water. It was further assumed that the rupture occurs to the element with the highest fuel temperature, the highest power density, and occurs immediately after continuous 1 MW operation. Therefore using these parameters provide very conservative (hypothetical worst case) results.

The MHA creates conditions far more severe than are actually possible. Therefore, the fact that the MHA consequences are within the 10 CFR Part 20 limits outside the reactor bay in the unrestricted area shows that the PSBR's operation is safe to the public. The emergency evacuation alarm which is initiated by the reactor bay radiation monitors and/or the bay air monitors will minimize the time the operation personnel spend in the reactor bay during the MHA to much less than the 7.5 minute time interval used in determining the consequences in the reactor bay. Therefore the operation personnel can also avoid any significant hazard from the MHA (within the 10 CFR Part 20 limits for radiation workers).

F. Reactivity Accident

In this accident, it is assumed that the reactor is taken to a 1.15 MW power level with the transient rod inserted in the core and then the reactor is pulsed with a \$3 reactivity insertion. This accident requires a breakdown in the PSBR Standard Operating Procedures, the overpower scrams, and a failure of the interlocks.

When the core is operating at 1.15 MW, its total reactivity has been reduced by more than \$4 depending on the average core fuel temperature. The measured fuel temperature in the B-ring using extrapolated experimental data for Core Loading 47^d with 95.5 elements would be 650 °C in the 12 wt% U fuel element, I-15. The maximum temperature will be slightly higher, but the fuel temperature near the cladding will be approximately half this temperature.

The maximum allowed core reactivity of \$7 leaves less than \$3 available for pulsing (actually the reactivity loss for Core Loading 47 would be = \$4.75 at 1.15 MW leaving only \$2.25 for a pulse).^e Should a \$2.25 pulse occur while the reactor is at 1.15 MW, the measured fuel temperature will rise from 650 °C to 1030 °C as calculated using the maximum measured \$2.25 pulse temperature^e for I-15 and Core Loading 47. In this case, when the core is pulsed from an initial power of 1.15 MW, the maximum fuel temperature is the measured fuel temperature. This is because the temperature rise during

^d Core Loading 47 is considered an extrema loading relative to steady state measured peak fuel temperatures.

^e These data are based on that obtained in 1994 & 1995.

a pulse has a different radial shape than that attained during steady state operation. During a pulse, the increase in fuel temperature is a maximum near the edge of the fuel. Superimposing this shape of the fuel temperature on that attained at a steady state power of 1.15 MW produces, at the end of the pulse, a relatively flat radial temperature distribution at approximately 1030 °C. However, since the negative temperature coefficient acts immediately as the transient rod moves upward, the final maximum fuel temperature will be less than 1030 °C. If the steady state fuel temperature is higher for a particular loading the reactivity loss due to temperature feedback is greater and the reactivity available for a pulse is subsequently less. Effectively the core excess reactivity limit also limits the maximum temperature of the fuel in this accident independent of the initial steady state fuel temperature. Therefore with the limit on the core excess reactivity the initial steady state core temperature and the maximum reactivity available for the accidental pulse work against each other (raising one lowers the other and conversely) to limit the final maximum fuel temperature to less than 1030 °C.

Administratively, if the reactor is operating above 900 kW all four control rods must be balanced. This implies that the transient rod would not be available for the \$2.25 pulse. In addition, the Technical Specification required pulse interlock (section 3.2.4), which prevents initiation of a pulse when reactor power is greater than 1 kW, will prevent the postulated accident. Also the Technical Specification required high power scrams will prevent operation at 1.15 MW. The result of the reactivity accident are peak fuel temperatures less than the safety limit of 1150 °C.

The \$5 ramp analysis was performed for AFRRI by General Atomics.⁽²⁴⁾ It indicated that even with a reactivity addition rate of \$2.50/second (averaged over the full rod travel) the safety limit (1150 °C) was not reached. The rod withdrawal was terminated with a high power scram less than 1 second into the event. A reactivity of \$1.86 was added after criticality was achieved and before the SCRAM occurred. The maximum power in the transient was 330 MW with a maximum fuel temperature of 330 °C. Compared to the above analyzed reactivity accident this excursion is inconsequential. It should be noted that the amount of reactivity available in the ramping rods does not impact on the final result as long as the reactivity addition rate does not exceed the \$2.50/second rate and the SCRAM time is not significantly longer than that analyzed.

G. Conclusion

There are two limits which, if not exceeded, will prevent rupture of the cladding of a TRIGA fuel element. They are:

1. Limit the fuel temperature to a maximum 1150 °C when the cladding temperature remains below 500 °C, i.e., when the fuel is covered with water.
2. Limit the fuel temperature to a maximum 950 °C when the cladding temperature is the same as the fuel temperature i.e., as with an air cooled core after a LOCA.

The Technical Specifications for the PSBR are established to prevent reaching these two limits. The 1150 °C temperature limit is not reached as the fuel temperatures are limited during pulse mode operations. Equation (34) provides a direct method for determining the maximum fuel temperature based on the measured fuel temperature during a pulse. Using this equation the following limits are established:

1. The maximum allowed reactivity insertion for the pulse mode and the maximum allowed worth of the pulse rod is \$3.50. A sudden insertion of \$3.50 excess reactivity results in a maximum peak fuel temperature of 1095 °C and a measured peak fuel temperature of 684 °C if the NP ≤ 2.2 .
2. With any core loading the maximum radial peaking factor, called the normalized power, NP, in the SAR is 2.2 if the transient rod worth is \$3.50. This ensures that a pulse with the full travel of the maximum allowed transient rod worth will not cause the fuel temperature in any fuel element to exceed the safety limit of 1150 °C. If the maximum allowed pulse is less than \$3.50 for any given core loading (i. e. the pulse can be limited by the worth of the transient rod, by the core excess, or administratively) the maximum NP can be increased as long as a calculation by an accepted method (documented in an administratively approved procedure) is done to show that the safety limit is not exceeded with the allowed pulse and NP. The limits shall be either physical or administrative or both.
3. The maximum allowed excess reactivity of the core is \$7. Thus, when the core is operating at 1.15 MW steady state, a maximum of \$2.25 of excess reactivity is available for pulsing, a minimum of \$4.75 of excess reactivity is needed to reach 1.15 MW. Based on core loading 47 and I-15 (an extrapolated measured fuel temperature of 650 °C) at 1.15 MW prior with a pulse insertion of \$2.25 (measured fuel temperature of 380 °C) the temperature would equal 1030 °C. However the Technical Specification required interlock prevents pulse initiation when the power is above 1 kW and the Technical Specification required high power SCRAMs prevent operation above 1.1 MW.
4. Core configuration limitations are also established to prevent a fuel element from producing too much power relative to the other fuel elements. The maximum elemental power density, ME^{PD}, allowed is 24.7 kW. If core size and or NP leads to a ME^{PD} greater than 24.7 kW when the reactor power is 1 MW the maximum allowed reactor power must be administratively reduced to reduce the ME^{PD} to 24.7 kW or less. The maximum allowed reactor power to maintain the ME^{PD} less than 24.7 kW for a given core configuration shall be determined by calculation by an accepted method (documented in an administratively approved procedure).

Limits set for steady state operation prevent the maximum fuel temperature reaching 1150 °C. Limits imposed here prevent the fuel temperature during a LOCA from reaching 950 °C. If operated at 1 MW continuously, a single fuel element could operate at its maximum power level of 24.7 kW and still not have its fuel temperature reach 950 °C during any conceived LOCA. In addition, the 24.7 kW ME^{PD} and the maximum measured fuel temperature of 650 °C during steady state operation limit the release of fission products such that the consequences are within the 10 CFR Part 20 limits if the cladding ruptures.

The MHA analyzes the effect of a fuel element cladding rupture in air after continuous operation at 1 MW. In addition, the reactor was assumed to have operated continuously during the previous year. Under these extreme conditions, the maximum TEDE to a person in the unrestricted area is 29 mrem after 1 hr and 30 mrem after 24 hr.

In conclusion, the analyses described in this section shows that under no possible accident conditions will the regulations in either 10 CFR Part 20 or 10 CFR Part 100 be violated. Thus, the PSBR can be operated safely within the regulatory limits.

H. References

1. Naughton, W.F., Cenko, M.J., Levine, S.H., and Witzig, W.F., "TRIGA Core Management Model," Nucl. Technology, vol. 23, p. 256 (Sept. 1974).
2. Naughton, W.F., Cenko, M.J., Levine, S.H., and Witzig, W.F., Increasing TRIGA Fuel Lifetime with 12 wt% U TRIGA Fuel, TOC-5, TRIGA Owner's Conference III (February 1974).
3. Haag, J.A., and Levine, S.H., "Thermal Analysis of The Pennsylvania State University Breazeale Nuclear Reactor," Nucl. Technology, vol. 19, p. 6 (July 1973).
4. Levine, S.H., Geisler, G.C., and Totenbier, R.E., Temperature Behavior of 12 wt% U TRIGA Fuel, TOC-5, TRIGA Owners' Conference III (February 1974).
5. Levine, S.H., Totenbier, R.E. (Penn State Univ.), and Ahmad T. Ali (PPAT Ismail - Malaysia), Fourteen Years of Fuel Management of the Penn State TRIGA Breazeale Reactor (PSBR), ANS Trans, vol. 33 (November 1979).
6. Levine, S.H. and H. Ocampo, "The k_{∞} -Meter Concept Verified via Subcritical/Critical TRIGA Experiments," Proceedings of the International Symposium on the Use and Development of Low and Medium Flux Research Reactors, MIT, Cambridge, MA (October 1983).
7. Kim, S.S. and S.H. Levine, "Verifying the Asymmetric Multiple Position Neutron Source (AMPNS) Method Using the TRIGA Reactor," Ninth TRIGA User's Conference, Anaheim, CA (March 1984).
8. Levine, S.H., "Module 5 - In-core Fuel Management," Nuclear Fuel Cycle Educational Module Series, N.D. Eckhoff, gen.ed., Kansas State University (July 1980).
9. Fowler, T.B., et.al., "EXTERMINATOR-II: A FORTRAN IV Code for Solving Multigroup Neutron Diffusion Equations in Two Dimensions," ORNL-4078, Oak Ridge National Laboratory (April 1967).
10. Huang, H.Y. and S.H. Levine, "An Automated Multiple-Cycle PWR Fuel Management Code," ANS Trans, (November 1978).
11. Cenko, M.J., "Comparison of PSBR Operation's History with the TRIGA Core Management Model," M.S. Thesis, The Pennsylvania State University (1972).
12. Barry, R.F., "LEOPARD - A Spectrum Dependent Non-Spatial Depletion Code for IBM-7094," WCAP-3269-26, Westinghouse Electric Corporation (September 1963).

13. Simnad, M. T., F. C. Foushie, and G. B. West, "Fuel Elements for Pulsed Reactors," GA Report E-117-393 (January 1975).
14. El-Wakil, M.M., "Nuclear Heat Transport," ANS (May 1978).
15. Goodwin, W.A., "The Measurement of Radial Power Distribution in a TRIGA Fuel Element During Reactor Excursion," Ph.D. Thesis, University of Illinois (1967).
16. Kim, S. S., "Development of an Asymmetric Multiple Position Neutron Source (AMPNS) Method for Monitoring the Criticality of the Degraded Reactor Core," Ph.D. Thesis, The Pennsylvania State University (1984).
17. PSBR Log Book 37, page 265 (November 21, 1984).
18. Shoptaugh, J. R., Jr., "Simulated Loss-of-Coolant Accident for TRIGA Reactors," GA-6596 (August 1965).
19. West, G. B., "Safety Analysis Report for the Torrey Pines TRIGA Mark III Reactor," GA-9064 (January 5, 1970).
20. Katcoff and Seymour, Nucleonics, vol. 18, p. 201 (November 1960).
21. Foushee and R. H. Peters "Summary of TRIGA Fuel Fission Product Release Experiments," GULF-EES-A10801 (September 1971).
22. Regulatory Guide 1.109, "Calculation of Annual Doses to Man From Routine Releases of Reactor Effluents for the Purpose of Evaluating Compliance With 10 CFR Part 50, Appendix I."
23. International Commission on Radiation Protection Report #. . .
24. General Atomics, *Analysis of 5 Dollar Ramp Insertion over 2 Second Interval in AFRR/ TRIGA™ Reactor*, General Atomics Publication of work performed for Armed Forces Radiobiological Research Institute, Bethesda, Maryland, April, 1988.
25. Coffey, C. O., Dee, J. B., Shoptaugh, Jr., J. R., West, G. B., and Whittemore, W. L., "Characteristics of Large Reactivity Insertions in a High Performance TRIGA U-ZrH Core," GA-6216, General Atomics (April 12, 1965).
26. W. F. Naughton, "Core Management Program to Optimize Fuel Utilization in TRIGA Research Reactors," Ph.D. Thesis, Nuclear Engineering Department, The Pennsylvania State University, University Park, Pennsylvania (September. 1972).
27. D. Hughes, P. Boyle, and S. H. Levine, "A New Management Plan for the Penn State TRIGA Reactor with Supporting Experiments and Calculations," Unpublished paper Nuclear Engineering Department, The Pennsylvania State University, University Park, Pennsylvania (Mar. 1996).

28. NUREG-1282, "Safety Evaluation Report on High-Uranium Content, Low -Enriched Uranium-Zirconium Hydride Fuels for TRIGA Reactors," Docket No. 50-163, U. S. Nuclear Regulatory Commission (August 1987).
29. M. T. Simnad, G. B. West, J. D. Randall, W. J. Richards, and D. Stahl, "Interpretation of Damage to the Flip Fuel During Operation of the Nuclear Science Center Reactor at Texas A&M University," GA-A16613, General Atomics (December, 1981).
30. M.T. Simnad, "The U-ZrHx Alloy: Its Properties and use in TRIGA Fuel," GA E-117-833, General Atomics (February, 1980).
31. Stationary Neutron Radiography System Final Safety Analysis Report prepared by Argoone National Laboratory, McClellan Air Force Base (January, 1992).